The Impact of Orbital Precession on Air-Sea CO\$_{2}\$ Exchange in the Southern Ocean

Cole Frederick Persch[1], Pedro DiNezio[1], and Nicole Suzanne Lovenduski[1]

[1]University of Colorado Boulder

April 16, 2023

Abstract

Orbital precession has been linked to glacial cycles and the atmospheric carbon dioxide (CO2) concentration, yet the direct impact of precession on the carbon cycle is not well understood. We analyze output from an Earth system model configured under different orbital parameters to isolate the impact of precession on air-sea CO2 flux in the Southern Ocean – a component of the global carbon cycle that is thought to play a key role on past atmospheric CO2 variations. Here, we demonstrate that periods of high precession are coincident with anomalous CO2 outgassing from the Southern Ocean. Under high precession, we find a poleward shift in the southern westerly winds, enhanced Southern Ocean meridional overturning, and an increase in the surface ocean partial pressure of CO2 along the core of the Antarctic Circumpolar Current. These results suggest that orbital precession may have played an important role in driving changes in atmospheric CO2

The Impact of Orbital Precession on Air-Sea CO_2 Exchange in the Southern Ocean

Cole F. Persch[1], **Pedro DiNezio**[1], **Nicole S. Lovenduski**[1,2]

[1]Department of Atmospheric and Oceanic Sciences, University of Colorado, Boulder, CO, USA
[2]Institute of Arctic and Alpine Research, University of Colorado, Boulder, CO, USA

Key Points:

- Increased insolation during austral summer due to orbital precession shifts the southern westerlies poleward.
- Poleward shifted westerlies enhance CO_2 outgassing due to increased turbulent exchanges and vertical transport of carbon-rich waters.
- Enhanced transport of carbon-rich waters is driven by a deepening of the overturning circulation in response to poleward shifted winds.

Corresponding author: Cole F. Persch, `cole.persch@colorado.edu`

Abstract

Orbital precession has been linked to glacial cycles and the atmospheric carbon dioxide (CO_2) concentration, yet the direct impact of precession on the carbon cycle is not well understood. We analyze output from an Earth system model configured under different orbital parameters to isolate the impact of precession on air-sea CO_2 flux in the Southern Ocean – a component of the global carbon cycle that is thought to play a key role on past atmospheric CO_2 variations. Here, we demonstrate that periods of high precession are coincident with anomalous CO_2 outgassing from the Southern Ocean. Under high precession, we find a poleward shift in the southern westerly winds, enhanced Southern Ocean meridional overturning, and an increase in the surface ocean partial pressure of CO_2 along the core of the Antarctic Circumpolar Current. These results suggest that orbital precession may have played an important role in driving changes in atmospheric CO_2.

1 Plain Language Summary

Over the past one million years, Earth has experienced several glacial and interglacial periods. As a glacial period is ending, carbon in the atmosphere can rise by up to 50%. The cause for this change is currently unknown, but most theories suggest that this carbon is released from the deep ocean into the atmosphere. The Southern Ocean surrounding Antarctica is the location of a lot of carbon outgassing from the deep ocean into the atmosphere, so it could be responsible for some of this change in atmospheric carbon. One of Earth's orbital cycles, precession, has been shown to change circulation in the Southern Ocean, that can affect how much carbon is carried from the deep ocean to the surface and released into the atmosphere. This paper uses simulations of a climate model to show that high precession corresponds to a 20% increase in the release of carbon from the Southern Ocean into the atmosphere. These findings suggest that precession could have affected changes in past atmospheric carbon concentrations.

2 Introduction

The Southern Ocean plays a central role in the global carbon cycle [*Marshall and Speer*, 2012]. The Southern Westerly Winds (SWW) interact with the ocean surface and force a zonally unbound meridional overturning circulation via Ekman transport, also known as *the Upper Cell* [*Speer et al.*, 2000]. On the poleward edge of this meridional overturning, deep, carbon-rich water is upwelled to the surface, and CO_2 is released into the atmosphere. Past studies have suggested that modern-day, interannual variability in the position and intensity of the SWW can invoke changes in Southern Ocean circulation, air-sea CO_2 flux, and atmospheric CO_2 concentration [*Lovenduski et al.*, 2007; *Butler et al.*, 2007; *Dufour et al.*, 2013; *Landschützer et al.*, 2019; *Nevison et al.*, 2020], and can influence the global carbon cycle [*Hauck et al.*, 2020].

The Southern Ocean likely played a key role in driving the large variations of atmospheric CO_2 observed over glacial-interglacial cycles [*Sigman et al.*, 2004; *Toggweiler et al.*, 2006; *Anderson et al.*, 2009]. This is because the Southern Ocean is one of the only places in the global ocean where dense ocean isopycnal surfaces outcrop, providing a means to connect the deep ocean interior to the atmosphere [*Rintoul et al.*, 2001]. However, the mechanisms responsible for changing air-sea CO_2 flux in the Southern Ocean on these timescales are not fully understood. In line with results from studies of modern-day Southern Ocean CO_2 flux variability, multiple manuscripts suggest that glacial-interglacial changes in the SWW may have played a role in some of these changes in air-sea CO_2 flux [*Toggweiler et al.*, 2006; *Menviel et al.*, 2008; *Tschumi et al.*, 2008; *Anderson et al.*, 2009; *d'Orgeville et al.*, 2010; *Lee et al.*, 2011; *Ai et al.*, 2020]. In these studies, the authors invoke SWW changes via mechanisms such as a global temperature increase [*Toggweiler et al.*, 2006], a cooling North Atlantic [*Anderson et al.*, 2009; *Lee et al.*, 2011], or variations in Earth's axial tilt (obliquity) [*Ai et al.*, 2020], yet no clear consensus on the cause of the SWW changes has emerged.

Recent studies suggest that the climate in the high-latitude Southern Hemisphere responds to orbital precession, one of the Milankovitch cycles with a spectral peak at ~21,000 years. Modelling and proxy studies have demonstrated that precession can significantly alter the position and strength of the SWW, which impacts circulation in the Southern Ocean [*Rutberg and Broccoli*, 2019; *Lamy et al.*, 2019]. Yet the models used in these studies are lacking a carbon cycle and thus are unable to predict if Southern Ocean air-sea CO_2 flux will be affected by precession.

Here, we use a state-of-the-art Earth system model which includes a respresentation of the carbon cycle to illustrate, for the first time, that orbital precession can have a marked impact on Southern Ocean air-sea CO_2 flux. We compare output from two simulations with different precessional states to illustrate the potential influence of precession on the Southern Ocean. As we will demonstrate, precession drives changes in the SWW and Southern Ocean circulation, alters the upwelling of deep, carbon-rich water, and produces anomalies in air-sea CO_2 flux. Our results suggest that orbital precession plays an important role in regulating atmospheric CO_2 concentrations, and provide a possible mechanism to explain the precessional peak in the ice core atmospheric CO_2 spectra.

3 Methods

Our primary numerical modeling tool is the low-resolution configuration of the Community Earth System Model (CESM) version 2.1.1 [*Danabasoglu et al.*, 2020], a fully coupled climate model designed for long climate integrations [*Shields et al.*, 2012]. The atmospheric component, CAM4, has a resolution of $\sim 3.75° \times 3.75°$ and 26 vertical levels [*Neale et al.*, 2013]. The ocean component, POP2, has nominal 2° latitude × 4° longitude resolution (lowering to less than 2° latitude resolution in the Southern Ocean), and 60 vertical levels [*Danabasoglu et al.*, 2012; *Smith et al.*, 2010]. POP2 represents subgrid-scale processes, such as mesoscale and submesoscale processes, via a collection of parameterizations [*Danabasoglu et al.*, 2008]. Importantly, the *Gent and Mcwilliams* [1990] mesoscale eddy parameterization includes a variable eddy-induced advection coefficient [*Gent*, 2016] which improves realism of eddy-driven mixing of carbon in the Southern Ocean at coarse resolution [*Lovenduski et al.*, 2013]. POP2 includes a biogeochemical model, MARBL [*Long et al.*, 2021]. MARBL contains multiple chemical tracers necessary for simulating ocean biogeochemistry such as carbon, nitrogen, phosphorus, iron, silicon, and oxygen.

Our experiment was designed to isolate the impact of precession on the Southern Ocean. We spun up CESM 2.1.1 for a 1000-year period with an eccentricity parameter of 0; since eccentricity modulates the strength of precession, this equilibration period had no precessional forcing. Carbon dioxide in the atmosphere is kept at a constant preindustrial value of 284.7 ppm. Over the last 500 years of the spinup, the globally integrated air-sea CO_2 flux drift is negligible ($-1.9 \pm 6.5 * 10^{-6}$ Pg C yr^{-2}; Figure S1). Following the spin-up period, two 100-year simulations were performed: the first, NoPrec, maintains an eccentricity parameter of 0, while the second, HighPrec, uses an eccentricity parameter of 0.058, which is the maximum value over the last one million years [*Laskar et al.*, 2004]. In the HighPrec simulation, the Northern Hemisphere summer solstice was configured to occur at the perihelion of Earth's orbit, which maximizes seasonal variability of insolation in the Southern Hemisphere. Our HighPrec simulation shows an immediate response of the SWW with minimal drift in global temperature consistent with the negligible effect of precession on annual mean insolation thus allowing us to use 100 years to study changes in the Southern Ocean.

While CESM2 is a well-validated model [*Danabasoglu et al.*, 2020; *Simpson et al.*, 2020; *Long et al.*, 2021], here we employ CESM2 components with lower resolution than the standard configuration, requiring an assessment of model validity at this resolution. Of particular interest in this study is the position and strength of the SWW. While the maximum zonal wind stress in the NoPrec SWW (0.14 N m^{-2}) agrees with modern estimates [*Large and Yeager*, 2009, 0.14 N m^{-2}], the modeled position of the SWW zonal wind stress (centered on 45°S) shows an equatorward bias relative to the estimated preindustrial value [*Large and Yeager*, 2009, centered on 53°S], which is a consequence of the lower resolution of the atmospheric model [*Shields et al.*, 2012]. The modelled position and strength of the SWW in our NoPrec simulation is within the range reported by models that participated in the Palaeoclimate Model Intercomparison Projects PMIP2 and PMIP3 under preindustrial conditions [*Rojas*, 2013], whose model components are simulated at a similar resolution as in our experiment. We find that the version of CESM2 employed in this study captures the air-sea fluxes of pre-industrial/natural CO_2 as compared to an observation-based inversion, as biome-mean CO_2 fluxes over the last 500 years of the spin-up simulation are within the uncertainty of the observation-based fluxes [*Mikaloff Fletcher et al.*, 2007] (Table S1).

A goal of this study is to isolate the different physical processes driving changes in air-sea CO_2 over the Southern Ocean. We approach this using the air-sea CO_2 equation as solved by the model:

$$F_{CO_2} = k_{sol} \times A_{noice} \times \Delta pCO_2 \times k_{gtv}, \tag{1}$$

where k_{sol} is the solubility of carbon in seawater, A_{noice} is the surface area without ice, ΔpCO_2 is the difference in the partial pressure of CO_2 between the surface ocean and the atmosphere, and k_{gtv} is the gas transfer velocity which is driven by surface winds [*Wanninkhof et al.*, 2013; *Wanninkhof*, 2014]. We isolate the contribution from each process as follows:

$$\delta[F]_{k_{sol}} = \delta[k_{sol}] \times A_{noice} \times \Delta pCO_2 \times k_{gtv}, \tag{2}$$

where $\delta[F]_{k_{sol}}$ isolates the impact of precession-driven changes in solubility (δk_{sol}) on air-sea CO_2 flux, δ corresponds to the difference between HighPrec and NoPrec, and the non-δ terms are derived from the NoPrec simulation.

We expanded this technique to include effects from changes in the covariance among the terms in Equation 1. Only one of these terms, the combination of ΔpCO_2 and k_{tur}, was significant relative to the changes computed using Equation 2. The influence of joint changes in these two processes was calculated as follows:

$$\delta[F]_{\Delta pCO_2, k_{gtv}} = k_{sol} \times A_{noice} \times \delta[\Delta pCO_2] \times \delta[k_{gtv}], \tag{3}$$

which isolates the impact of simultaneous, precession-driven changes in both ΔpCO_2 and k_{tur}. It is important to note that since CO_2 in the atmosphere is kept constant, the ΔpCO_2 term in the air-sea CO_2 flux decomposition corresponds to only changes in surface ocean pCO_2. The surface ocean pCO_2 changes are further broken down into contributions from temperature, salinity, Dissolved Inorganic Carbon (DIC), alkalinity, and freshwater forcing.

In this manuscript, we emphasize orbital precession-driven changes in the Southern Ocean, calculated as the difference between the century-mean values in the 100-year HighPrec simulation and the 100-year NoPrec simulation. This difference (δ) is reported to be statistically significant at the 99% level if it exceeds 2.58 times the NoPrec temporal standard deviation, assuming a normal distribution.

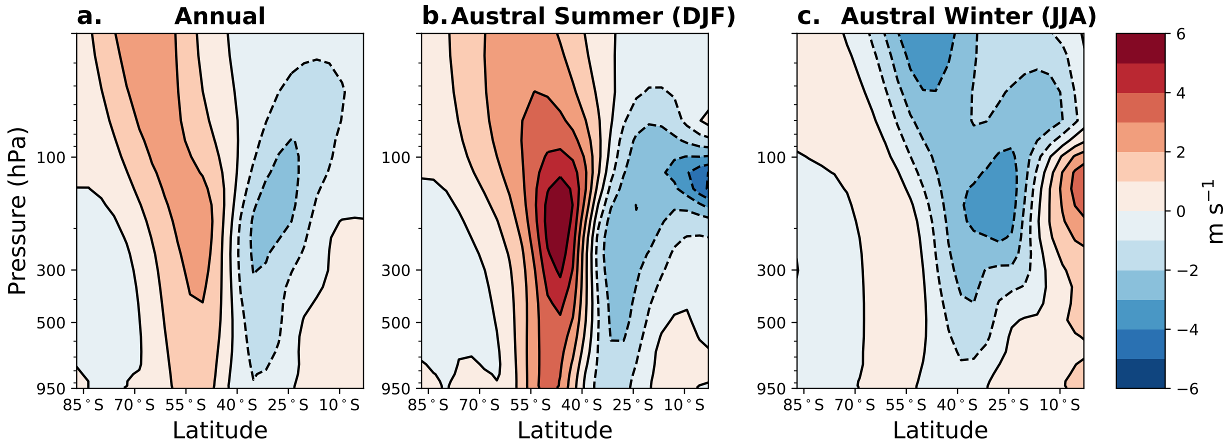

Figure 1. Precession-driven anomalies in Southern Hemisphere zonal-mean wind speed (m s^{-1}), calculated as the century-mean difference from the HighPrec and NoPrec simulations. (a) Annual-mean anomalies, (b) Austral summer (DJF) anomalies, and (c) Austral winter (JJA) anomalies. Positive values/contours correspond to westerly wind anomalies.

4 Results

Our simulations show that high precession produces a shift in the SWW that manifests most strongly in the austral summer relative to conditions with no precessional forcing. In the summer months (DJF), we find a ∼6 m s^{-1} increase in the zonal-mean wind speed extending from 300 to 100 hPa and centered at 50°S; we also find a ∼3 m s^{-1} decrease at the same heights centered on 30°S (Figure 1b). Whereas, in the winter months (JJA), high precession leads to a general weakening of the SWW in JJA (Figure 1c). The shift in the SWW during the DJF season exceeds the SWW weakening in the JJA season, resulting in an annual mean shift (Figure 1a). This poleward shift in the SWW appears throughout the entire vertical structure of the atmosphere, indicating a poleward intensification of the surface westerlies that drive Southern Ocean circulation.

The simulated precessional shift in the SWW corresponds to large deviations in the atmospheric temperature structure. We find that the strongest temperature anomalies occur during the DJF season, due to austral summer receiving significantly more insolation in periods of high precession (Figure S2). We find a precession-driven increase in the pole-to-Equator temperature gradient around 200 hPa in both the annual-mean and DJF zonal-mean temperature profiles (Figure S2g,h) that corresponds to the greatest wind anomalies (Figure 1a,b). These findings indicate that periods of high precession, or periods when the perihelion of Earth's orbit occur at the Southern Hemisphere summer solstice, are associated with an enhanced pole-to-Equator temperature gradient at the approximate position of the tropopause.

Carbon outgassing in the Southern Ocean increases by approximately 20% in HighPrec relative to NoPrec. The century-mean, integrated (<35°S) air-sea CO_2 flux increases from 0.264 Pg C yr^{-1} in NoPrec to 0.322 Pg C yr^{-1} in HighPrec. This precession-driven anomalous air-sea CO_2 flux is most pronounced in the Indian and Pacific sectors of the Southern Ocean: regions typically characterized by outgassing or weak uptake of CO_2 (Figure 2). North of the ACC streamlines, and in the Atlantic sector of the ACC, high precession is associated with anomalous uptake of CO_2 (Figure 2). The precession-driven anomalous outgassing exceeds the anomalous uptake, such that the Southern Ocean be-

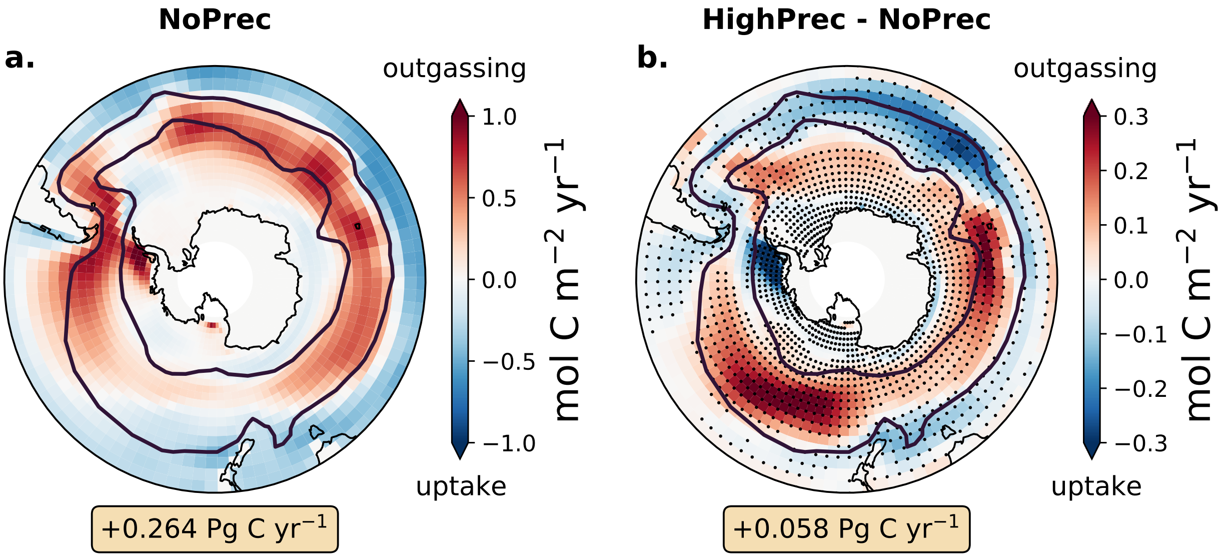

Figure 2. (a) Century-mean sea-air CO_2 flux from the NoPrec simulation. (b) Precession-driven change in sea-air CO_2 flux, calculated as the difference in century-mean CO_2 flux from the HighPrec and NoPrec simulations. Stippling indicates a statistically significant difference at the 99% confidence level. Units are mol C m^{-2} yr^{-1}, and positive values correspond to CO_2 outgassing. Black lines show the Antarctic Circumpolar Current (ACC) in the NoPrec simulation, bound by the 7 Sv and 100 Sv barotropic streamlines. Numbers under each map indicate the Southern Ocean (<35°S) integrated flux and anomalous flux, respectively (Pg C yr^{-1}).

comes a larger net source of CO_2 to the atmosphere under high precession relative to no precession.

The precession-driven increase in Southern Ocean sea-air CO_2 flux is a result of changes in both surface ocean pCO_2 and the gas transfer velocity caused by changes in precession. We isolated the influence of each physical process driving changes in air-sea flux using the technique outlined in Methods. We find that the spatial pattern of the changes in CO_2 flux is driven by the contribution from ΔpCO_2 (determined by surface ocean pCO_2 since carbon in the atmosphere is constant) (Figure 3), which itself is impacted by changing surface ocean DIC (Figure S3). This indicates that the surface ocean pCO_2 response to precession drives the anomalous outgassing in the Indian and Pacific sectors of the ACC and the anomalous uptake in the Atlantic sector of the ACC. When integrated over the Southern Ocean (<35°S), the large magnitude positive and negative ΔpCO_2 anomalies nearly balance, such that the net contribution to the integrated flux difference is small (0.019 Pg C yr^{-1}; Figure 3d). The precession-driven CO_2 flux difference is also strongly affected by the simultaneous changes in the gas transfer velocity and ΔpCO_2, which contribute to enhanced outgassing in the ACC and a large, positive Southern Ocean integrated flux contribution (0.091 Pg C yr^{-1}; Figure 3f). The changes in gas transfer velocity contributes a moderate decrease in carbon outgassing of -0.038 Pg C yr^{-1} (Figure 3e). Whereas, the changes in air-sea CO_2 flux due to sea ice extent (Figure 3b) and solubility (Figure 3c) have minimal impacts on the flux difference, with the exception of sea ice extent near the West Antarctic Peninsula which drives localized anomalous CO_2 uptake (Figure 3b).

The core of the Southern Ocean meridional overturning circulation shifts poleward and deepens under high precession, tapping into a richer carbon source explaining the

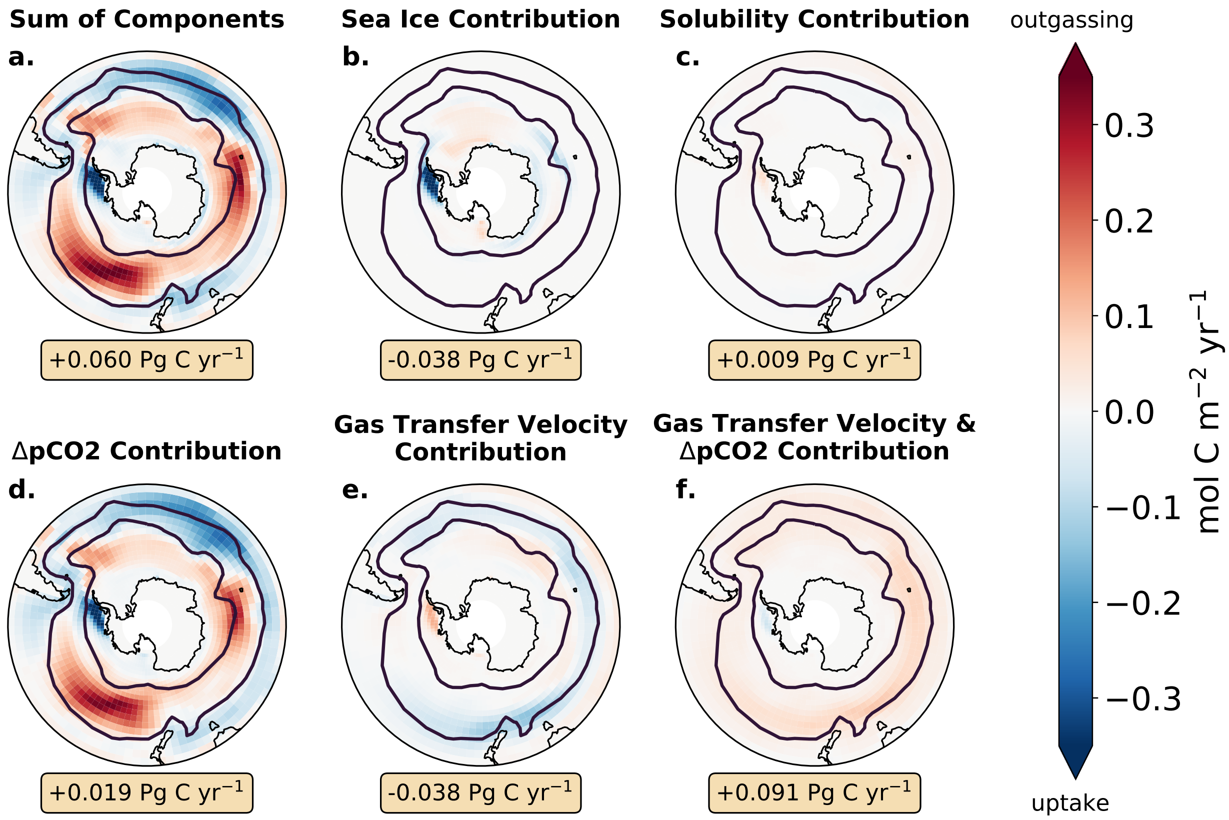

Figure 3. Contribution of (b) sea ice extent, (c) solubility, (d) ΔpCO_2, (e) gas transfer velocity, and (f) the combination of gas transfer velocity and ΔpCO_2 change to the total air-sea CO_2 flux difference (mol C m^{-2} yr^{-1}) due to precession. Contributions calculated as in Equation 2 and Equation 3 using the century-mean differences in each variable from the HighPrec and NoPrec simulations. (a) Shows the sum of the five components (b-f), which is nearly identical to Figure 2. Black lines show the Antarctic Circumpolar Current (ACC) in the NoPrec simulation, bound by the 7 Sv and 100 Sv barotropic streamlines. Numbers under each map indicate the Southern Ocean (<35°S) integrated contribution to the anomalous flux (Pg C yr^{-1}).

increase in surface pCO_2. Relative to the NoPrec simulation, both the wind stress and overturning maxima shift southward by $\sim 1°$ in the HighPrec simulation (Figure 4). In its more poleward position, the meridional overturning circulation streamlines intersect waters with higher DIC concentrations (Figure 4b). For example, the 20 Sv streamline in the NoPrec simulation intersects waters only up to 1250 meters deep with maximum DIC concentrations of $\sim$2330 mmol m^{-3}. In contrast, this streamline reaches a deeper depth of 1500 meters in the HighPrec simulation overlapping with higher DIC concentration of $\sim$2340 mmol m^{-3} (Figure 4). This shifted and deepened meridional overturning increases the amount of carbon that is brought to the surface in HighPrec relative to NoPrec, which is a key component (Figure S3) of the simulated increase in CO_2 outgassing.

The largest increases in air-sea CO_2 flux occur where precession drives both enhanced gas exchange velocities and anomalous meridional and vertical advection of carbon-rich water (Figures 2, 3, 4, S4). High precession is associated with increases in the modeled air-sea gas transfer velocity, k_{gtv}, near the northern core of the ACC; these increases are especially pronounced in the Indian and western Pacific sectors (Figure S4)a). The SWW changes that induce increases in near surface turbulence and air-sea gas exchange also alter the ocean circulation (Figure 4), driving increases in surface ocean DIC and pCO_2 in the Indian and western Pacific sectors of the ACC (Figures S4b, S3a). Where the gas transfer velocity and pCO_2 anomalies align, they combine to produce enhanced CO_2 outgassing (Figures 2b, 4).

5 Conclusions and Discussion

Our study demonstrates that high precessional states impact key Southern Ocean processes involved in the global carbon cycle, ultimately leading to a substantial increase in sea-air CO_2 flux. Under high precessional forcing of the Southern Hemisphere, our model predicts a $\sim 1°$ poleward shift of the SWW across the troposphere, likely caused by insolation-driven atmospheric temperature changes over Antarctica. The associated poleward shift in the SWW drives a stronger and deeper meridional overturning circulation, enhancing the vertical and lateral advection of carbon-rich water. The shifted SWW also increase turbulent air-sea exchange which combined with the changes ocean overturning combine to produce a 20% increase in CO_2 outgassing from the Southern Ocean.

The precession-driven poleward shift in the SWW predicted by our model strongly resembles a positive phase of the Southern Annular Mode [SAM; see, e.g., Figure 7 of *Thompson et al.*, 2000], albeit with a different seasonality. While the SAM pattern has been linked to internal climate variability and anthropogenic forcing, here we demonstrate that the Southern Hemisphere seasonal insolation changes associated with precession produce a similar shift in the SWW. The simulated change in the equator-to-pole temperature gradient in the upper troposphere is similar to that of the positive SAM phase, when the polar atmosphere shows cooling aloft associated with Ozone forcing [see Figure 8 of *Thompson et al.*, 2000]. Periods of high precession shift and deepen the meridional overturning circulation in our model (Figure 4b), which has also been found to occur during positive phases of the SAM [*Yang et al.*, 2007]. Thus, results from our simulations suggest that the Southern Hemisphere response to precessional forcing exhibits similar features to the Southern Hemisphere response to variability associated with the SAM, suggesting that past changes could be used to understand ongoing changes in Southern Hemisphere climate.

The precession-driven changes in ocean meridional overturning and air-sea CO_2 flux that we report broadly agree with other modeling studies that directly test the response of the Southern Ocean to changes in the magnitude and position of the SWWs [*Menviel et al.*, 2008; *Tschumi et al.*, 2008; *d'Orgeville et al.*, 2010]. While these studies are focused on shifts in the winds caused by a combination of orbital forcing changes on glacial-

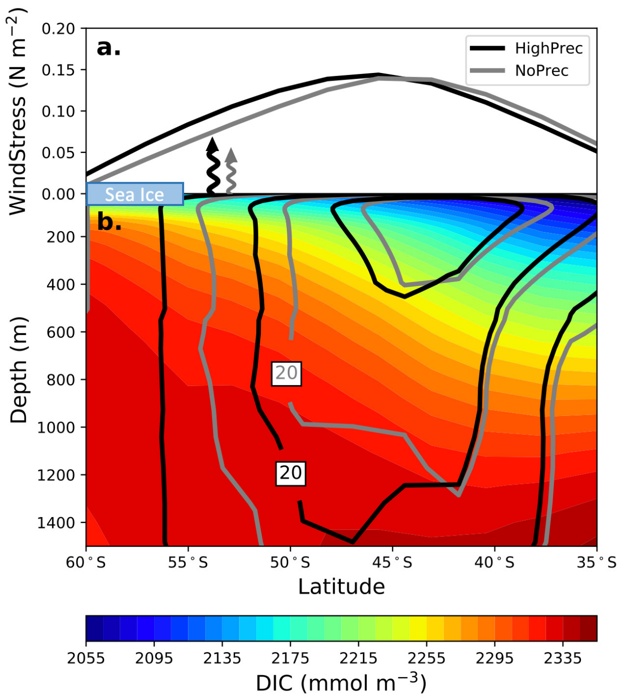

Figure 4. Southern Ocean response to high precession. (a) Century-mean zonal-mean surface wind stress from (gray) the NoPrec simulation and (black) the HighPrec simulation. (b) Century-mean (colors) zonal-mean DIC concentration from the HighPrec simulation with meridional overturning streamlines from the (gray) NoPrec simulation and (black) HighPrec simulation. Overturning units are Sv with contour lines every 10 Sv; positive streamlines indicate clockwise flow. Squiggly arrows indicate the relative position and strength in the annual peak carbon outgassing in both simulations.

to-interglacial timescales, our study demonstrates that orbital precession alone can induce changes in the SWW and thus air-sea CO_2 flux.

Our study uses an Earth system model that is configured with relatively coarse horizontal resolution in the atmosphere and ocean model components to support long integrations potentially affect the realism of our results. The average annual peak in zonal-mean wind stress occurs at 45°S in our model. While this shows good agreement with other models that have similar horizontal resolution [see Figure 3 of *Shields et al.*, 2012], this position is equatorward relatove to the modern-day position of 53° *Large and Yeager* [2009]. Similar poleward shift in the position of the SWW in response to high precession is also found in other modeling studies with higher resolution, suggesting our results are not model dependent For instance, *Rutberg and Broccoli* [2019] used a model with a resolution of 2° latitude by 2.5° longitude in the atmosphere and found a poleward shift of 4° between extreme precessional states. The coarse resolution of our ocean model component requires that processes influenced by mesoscale eddies are parameterized. Numerous studies have emphasized the importance of mesoscale eddies in Southern Ocean meridional overturning, especially in its response to changes in surface wind stress [*Marshall and Radko*, 2003; *Hallberg and Gnanadesikan*, 2006; *Abernathey et al.*, 2011; *Marshall and Speer*, 2012; *Doddridge et al.*, 2019]. Our model uses a variable eddy-induced advection coefficient [*Gent*, 2016], which has been shown to capture the sensitivity of these unresolved processes to changes in circulation [*Lovenduski et al.*, 2013]. Indeed, results from our model indicate that the eddy-induced meridional overturning circulation strengthens in response to SWW changes under high precession (counterclockwise anomalies in Figure S5b), suggesting that our coarse resolution ocean model component is capable of capturing changes in unresolved eddy advection. Future work should explore the responses identified here using higher resolution configuration of capable of resolving these processes.

Taken together, our findings imply that orbital precession plays an important role in regulating atmospheric carbon dioxide concentration through its effect on the Southern Ocean. While our study is focused on the impact of precession on Southern Ocean CO_2 fluxes, it is reasonable to expect that other regions in the coupled, global Earth system could also be affected by changes in precession. Future studies should address whether precession produces anomalous air-sea CO_2 fluxes in other regions of the global ocean, and whether the global ocean carbon reservoir grows or shrinks in response to precession. As we have demonstrated, the changes in seasonal insolation associated with orbital precession could have driven to a shift in the position of the westerly winds over the Southern Ocean, increasing the upwelling of carbon-rich water to the surface exchanging more carbon with the atmosphere. This mechanism could explain variability in ice core records of atmospheric CO_2 variability on precessional timescales [*Petit et al.*, 1999].

Open Research

The analysis data of the CESM simulation in this study were uploaded to https://doi.org/10.5281/zenodo.7761019.

Acknowledgments

This research was supported by the National Science Foundation (OCE-2043447 to PD and CP and OCE-1752724, OCE-1948664, and FRES-2021648 to NL). NCAR is sponsored by the National Science Foundation. Computational facilities have been provided by the Climate Simulation Laboratory, which is managed by CISL at NCAR.

References

Abernathey, R., J. Marshall, and D. Ferreira (2011), The dependence of southern ocean meridional overturning on wind stress, *Journal of Physical Oceanography*, *41*(12), 2261–2278.

Ai, X. E., A. S. Studer, D. M. Sigman, A. Martínez-García, F. Fripiat, L. M. Thöle, E. Michel, J. Gottschalk, L. Arnold, S. Moretti, et al. (2020), Southern ocean upwelling, earth's obliquity, and glacial-interglacial atmospheric co2 change, *Science*, *370*(6522), 1348–1352.

Anderson, R., S. Ali, L. Bradtmiller, S. Nielsen, M. Fleisher, B. Anderson, and L. Burckle (2009), Wind-driven upwelling in the southern ocean and the deglacial rise in atmospheric co2, *science*, *323*(5920), 1443–1448.

Butler, A. H., D. W. Thompson, and K. R. Gurney (2007), Observed relationships between the southern annular mode and atmospheric carbon dioxide, *Global Biogeochemical Cycles*, *21*(4).

Danabasoglu, G., R. Ferrari, and J. C. McWilliams (2008), Sensitivity of an ocean general circulation model to a parameterization of near-surface eddy fluxes, *Journal of Climate*, *21*(6), 1192–1208.

Danabasoglu, G., S. C. Bates, B. P. Briegleb, S. R. Jayne, M. Jochum, W. G. Large, S. Peacock, and S. G. Yeager (2012), The ccsm4 ocean component, *Journal of Climate*, *25*(5), 1361–1389.

Danabasoglu, G., J.-F. Lamarque, J. Bacmeister, D. Bailey, A. DuVivier, J. Edwards, L. Emmons, J. Fasullo, R. Garcia, A. Gettelman, et al. (2020), The community earth system model version 2 (cesm2), *Journal of Advances in Modeling Earth Systems*, *12*(2), e2019MS001,916.

Doddridge, E. W., J. Marshall, H. Song, J.-M. Campin, M. Kelley, and L. Nazarenko (2019), Eddy compensation dampens southern ocean sea surface temperature response to westerly wind trends, *Geophysical Research Letters*, *46*(8), 4365–4377.

d'Orgeville, M., W. Sijp, M. England, and K. Meissner (2010), On the control of glacial-interglacial atmospheric co2 variations by the southern hemisphere westerlies, *Geophysical Research Letters*, *37*(21).

Dufour, C. O., J. L. Sommer, M. Gehlen, J. C. Orr, J.-m. Molines, J. Simeon, and B. Barnier (2013), Eddy compensation and controls of the enhanced sea-to-air co2 flux during positive phases of the southern annular mode, *Global Biogeochemical Cycles*, *27*(3), 950–961.

Gent, P. R. (2016), Effects of southern hemisphere wind changes on the meridional overturning circulation in ocean models, *Annual review of marine science*, *8*, 79–94.

Gent, P. R., and J. C. Mcwilliams (1990), Isopycnal mixing in ocean circulation models, *Journal of Physical Oceanography*, *20*(1), 150–155.

Hallberg, R., and A. Gnanadesikan (2006), The role of eddies in determining the structure and response of the wind-driven southern hemisphere overturning: Results from the modeling eddies in the southern ocean (meso) project, *Journal of Physical Oceanography*, *36*(12), 2232–2252.

Hauck, J., M. Zeising, C. Le Quéré, N. Gruber, D. C. Bakker, L. Bopp, T. T. T. Chau, Ö. Gürses, T. Ilyina, P. Landschützer, et al. (2020), Consistency and challenges in the ocean carbon sink estimate for the global carbon budget, *Frontiers in Marine Science*, *7*, 571,720.

Lamy, F., J. C. Chiang, G. Martínez-Méndez, M. Thierens, H. W. Arz, J. Bosmans, D. Hebbeln, F. Lambert, L. Lembke-Jene, and J.-B. Stuut (2019), Precession modulation of the south pacific westerly wind belt over the past million years, *Proceedings of the National Academy of Sciences*, *116*(47), 23,455–23,460.

Landschützer, P., T. Ilyina, and N. S. Lovenduski (2019), Detecting regional modes of variability in observation-based surface ocean p co2, *Geophysical Research Let-*

ters, *46*(5), 2670–2679.
Large, W., and S. Yeager (2009), The global climatology of an interannually varying air–sea flux data set, *Climate dynamics*, *33*, 341–364.
Laskar, J., P. Robutel, F. Joutel, M. Gastineau, A. Correia, and B. Levrard (2004), A long-term numerical solution for the insolation quantities of the earth, *Astronomy & Astrophysics*, *428*(1), 261–285.
Lee, S.-Y., J. C. Chiang, K. Matsumoto, and K. S. Tokos (2011), Southern ocean wind response to north atlantic cooling and the rise in atmospheric co2: Modeling perspective and paleoceanographic implications, *Paleoceanography*, *26*(1).
Long, M. C., J. K. Moore, K. Lindsay, M. Levy, S. C. Doney, J. Y. Luo, K. M. Krumhardt, R. T. Letscher, M. Grover, and Z. T. Sylvester (2021), Simulations with the marine biogeochemistry library (marbl), *Journal of Advances in Modeling Earth Systems*, *13*(12), e2021MS002,647.
Lovenduski, N. S., N. Gruber, S. C. Doney, and I. D. Lima (2007), Enhanced co2 outgassing in the southern ocean from a positive phase of the southern annular mode, *Global Biogeochemical Cycles*, *21*(2).
Lovenduski, N. S., M. C. Long, P. R. Gent, and K. Lindsay (2013), Multi-decadal trends in the advection and mixing of natural carbon in the southern ocean, *Geophysical Research Letters*, *40*(1), 139–142.
Marshall, J., and T. Radko (2003), Residual-mean solutions for the antarctic circumpolar current and its associated overturning circulation, *Journal of Physical Oceanography*, *33*(11), 2341–2354.
Marshall, J., and K. Speer (2012), Closure of the meridional overturning circulation through southern ocean upwelling, *Nature Geoscience*, *5*(3), 171–180.
Menviel, L., A. Timmermann, A. Mouchet, and O. Timm (2008), Climate and marine carbon cycle response to changes in the strength of the southern hemispheric westerlies, *Paleoceanography*, *23*(4).
Mikaloff Fletcher, S., N. Gruber, A. R. Jacobson, M. Gloor, S. Doney, S. Dutkiewicz, M. Gerber, M. Follows, F. Joos, K. Lindsay, et al. (2007), Inverse estimates of the oceanic sources and sinks of natural co2 and the implied oceanic carbon transport, *Global Biogeochemical Cycles*, *21*(1).
Neale, R. B., J. Richter, S. Park, P. H. Lauritzen, S. J. Vavrus, P. J. Rasch, and M. Zhang (2013), The mean climate of the community atmosphere model (cam4) in forced sst and fully coupled experiments, *Journal of Climate*, *26*(14), 5150–5168.
Nevison, C. D., D. R. Munro, N. S. Lovenduski, R. F. Keeling, M. Manizza, E. J. Morgan, and C. Rödenbeck (2020), Southern annular mode influence on wintertime ventilation of the southern ocean detected in atmospheric o2 and co2 measurements, *Geophysical Research Letters*, *47*(4), e2019GL085,667.
Petit, J.-R., J. Jouzel, D. Raynaud, N. I. Barkov, J.-M. Barnola, I. Basile, M. Bender, J. Chappellaz, M. Davis, G. Delaygue, et al. (1999), Climate and atmospheric history of the past 420,000 years from the vostok ice core, antarctica, *Nature*, *399*(6735), 429–436.
Rintoul, S. R., C. W. Hughes, and D. Olbers (2001), The antarctic circumpolar current system, in *International Geophysics*, vol. 77, pp. 271–XXXVI, Elsevier.
Rojas, M. (2013), Sensitivity of southern hemisphere circulation to lgm and 4× co2 climates, *Geophysical Research Letters*, *40*(5), 965–970.
Rutberg, R., and A. Broccoli (2019), Response of the high-latitude southern hemisphere to precessional forcing: Implications for pleistocene ocean circulation, *Paleoceanography and paleoclimatology*, *34*(7), 1092–1106.
Shields, C. A., D. A. Bailey, G. Danabasoglu, M. Jochum, J. T. Kiehl, S. Levis, and S. Park (2012), The low-resolution ccsm4, *Journal of Climate*, *25*(12), 3993–4014.
Sigman, D. M., S. L. Jaccard, and G. H. Haug (2004), Polar ocean stratification in a cold climate, *Nature*, *428*(6978), 59–63.

Simpson, I. R., J. Bacmeister, R. B. Neale, C. Hannay, A. Gettelman, R. R. Garcia, P. H. Lauritzen, D. R. Marsh, M. J. Mills, B. Medeiros, et al. (2020), An evaluation of the large-scale atmospheric circulation and its variability in cesm2 and other cmip models, *Journal of Geophysical Research: Atmospheres*, *125*(13), e2020JD032,835.

Smith, R., P. Jones, B. Briegleb, F. Bryan, G. Danabasoglu, J. Dennis, J. Dukowicz, C. Eden, B. Fox-Kemper, P. Gent, et al. (2010), The parallel ocean program (pop) reference manual ocean component of the community climate system model (ccsm) and community earth system model (cesm), *LAUR-01853*, *141*, 1–140.

Speer, K., S. R. Rintoul, and B. Sloyan (2000), The diabatic deacon cell, *Journal of physical oceanography*, *30*(12), 3212–3222.

Thompson, D. W., J. M. Wallace, and G. C. Hegerl (2000), Annular modes in the extratropical circulation. part ii: Trends, *Journal of climate*, *13*(5), 1018–1036.

Toggweiler, J. R., J. L. Russell, and S. R. Carson (2006), Midlatitude westerlies, atmospheric co2, and climate change during the ice ages, *Paleoceanography*, *21*(2).

Tschumi, T., F. Joos, and P. Parekh (2008), How important are southern hemisphere wind changes for low glacial carbon dioxide? a model study, *Paleoceanography*, *23*(4).

Wanninkhof, R. (2014), Relationship between wind speed and gas exchange over the ocean revisited, *Limnology and Oceanography: Methods*, *12*(6), 351–362.

Wanninkhof, R., G.-H. Park, T. Takahashi, C. Sweeney, R. Feely, Y. Nojiri, N. Gruber, S. C. Doney, G. A. McKinley, A. Lenton, et al. (2013), Global ocean carbon uptake: magnitude, variability and trends, *Biogeosciences*, *10*(3), 1983–2000.

Yang, X.-Y., D. Wang, J. Wang, and R. X. Huang (2007), Connection between the decadal variability in the southern ocean circulation and the southern annular mode, *Geophysical Research Letters*, *34*(16).

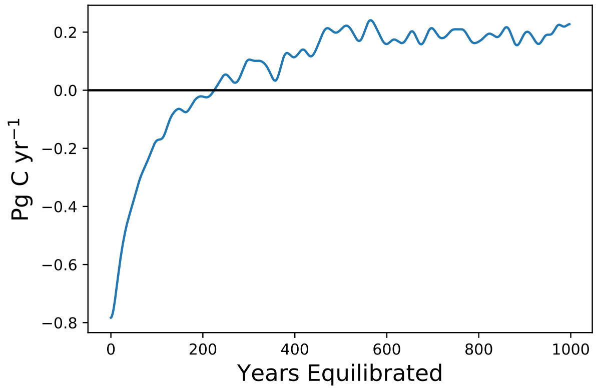

Figure S1. Globally integrated sea-air CO_2 flux during the model spin-up. High-frequency variability has been removed using a σ=10 Gaussian filter.

Region	Model spin-up	*Mikaloff Fletcher et al.* [2007]
Polar S. Ocean	0.10 ±0.03	0.04 ±0.04
Sub-Polar Pac. & Ind.	0.31 ±0.08	0.25 ±0.09
Sub-Polar Atl.	0.11 ±0.03	0.11 ±0.05

Table S1. Spatially integrated air-sea CO_2 flux (Pg C yr^{-1}) in three Southern Ocean regions averaged over the last 500 years of the model spin-up, and the natural air-sea CO_2 flux reported in *Mikaloff Fletcher et al.* [2007].

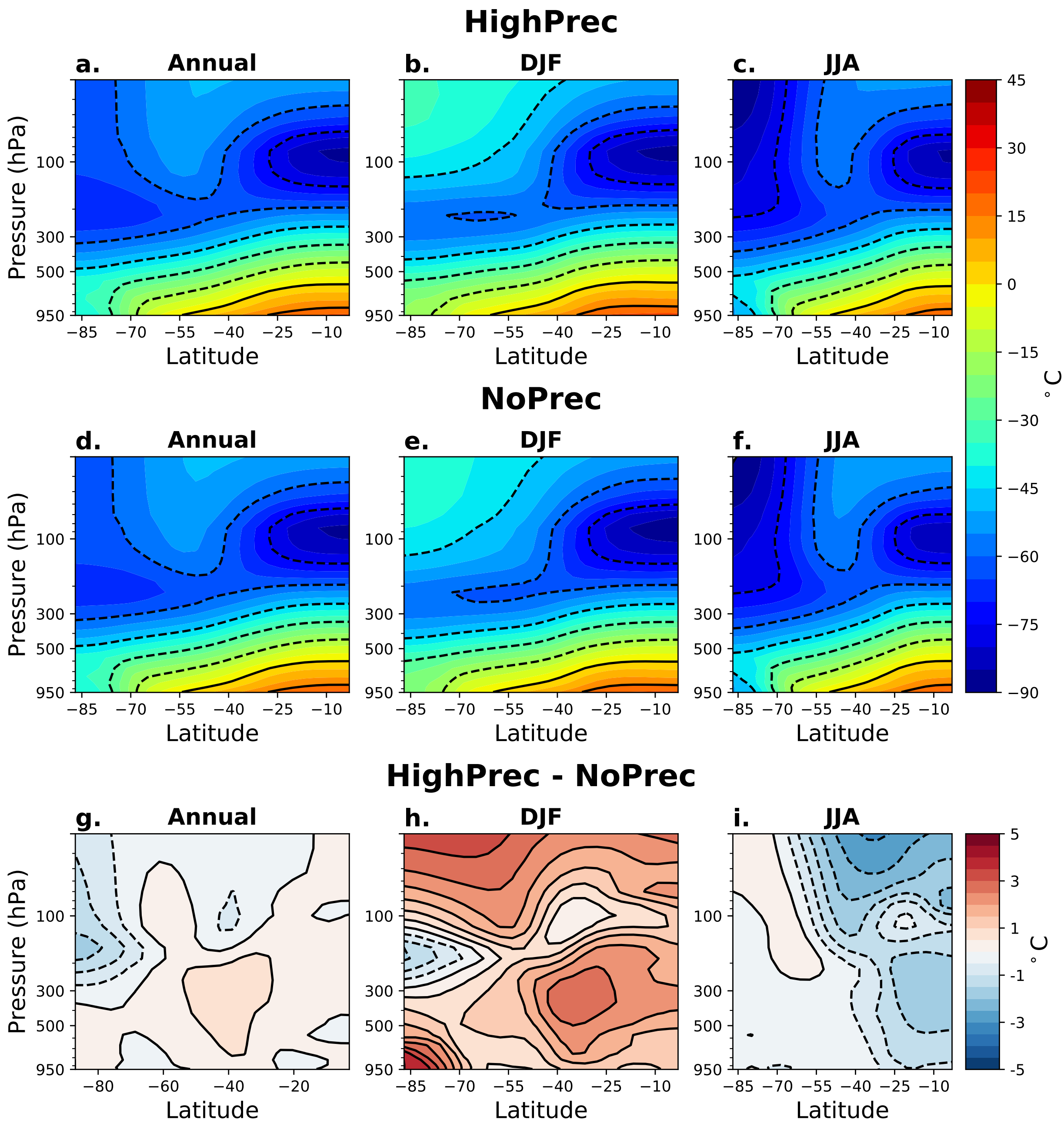

Figure S2. Zonal-mean atmospheric temperature for (1^{st} column) annual-mean, (2^{nd} column) Austral summer (DJF), and (3^{rd} column) Austral winter (JJA) periods in the (1^{st} row) HiPrec and (2^{nd} row) NoPrec simulations (°C). (3^{rd} row) Precession-driven anomalies in zonal-mean atmospheric temperature, calculated as the century-mean difference from the HighPrec and NoPrec simulations.

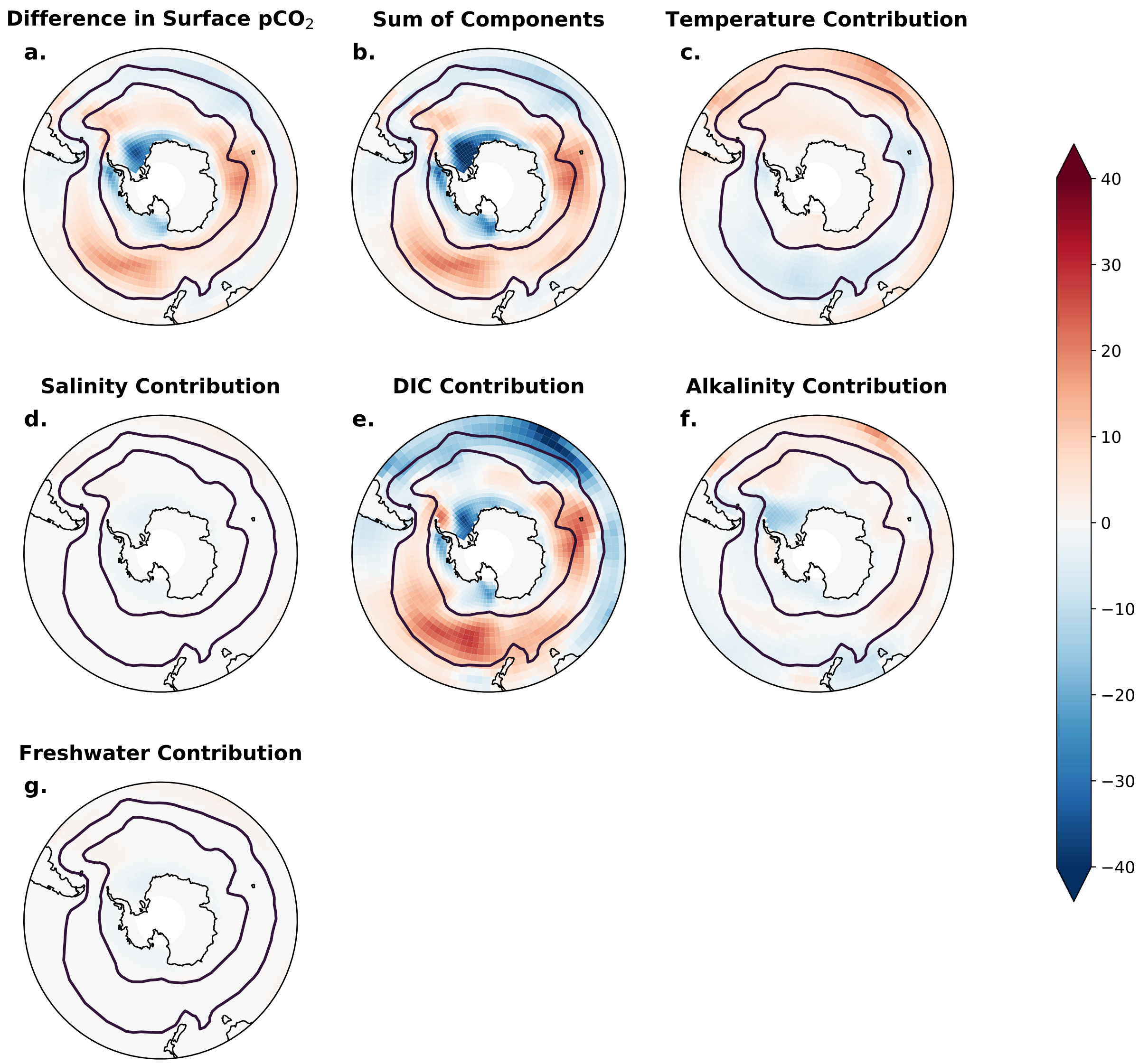

Figure S3. Contribution of (c) temperature, (d) salinity, (e) DIC, (e) Alkalinity, and (f) freshwater anomalies to the total surface ocean pCO_2 (ppmv) difference due to precession. The contributions of each variable responsible for driving surface ocean pCO_2 were calculated using the century-mean differences in each variable from the HighPrec and NoPrec simulations [see Equation 3 of *Lovenduski et al.*, 2007]. (b) Shows the sum of the five components (c-g). Black lines show the Antarctic Circumpolar Current (ACC) in the NoPrec simulation, bound by the 7 Sv and 100 Sv barotropic streamlines.

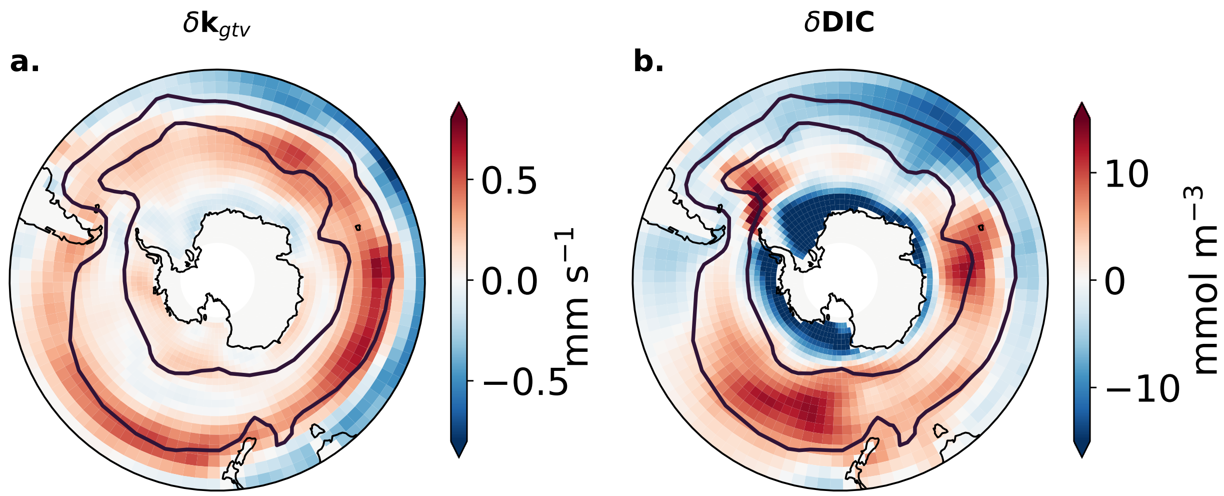

Figure S4. Precession-driven changes in (a) air-sea gas transfer velocity (mm s^{-1}), and (b) surface ocean DIC (mmol m^{-3}), calculated as the difference in century-means from the HighPrec and NoPrec simulations. Black lines show the Antarctic Circumpolar Current (ACC) in the No-Prec simulation, bound by the 7 Sv and 100 Sv barotropic streamlines.

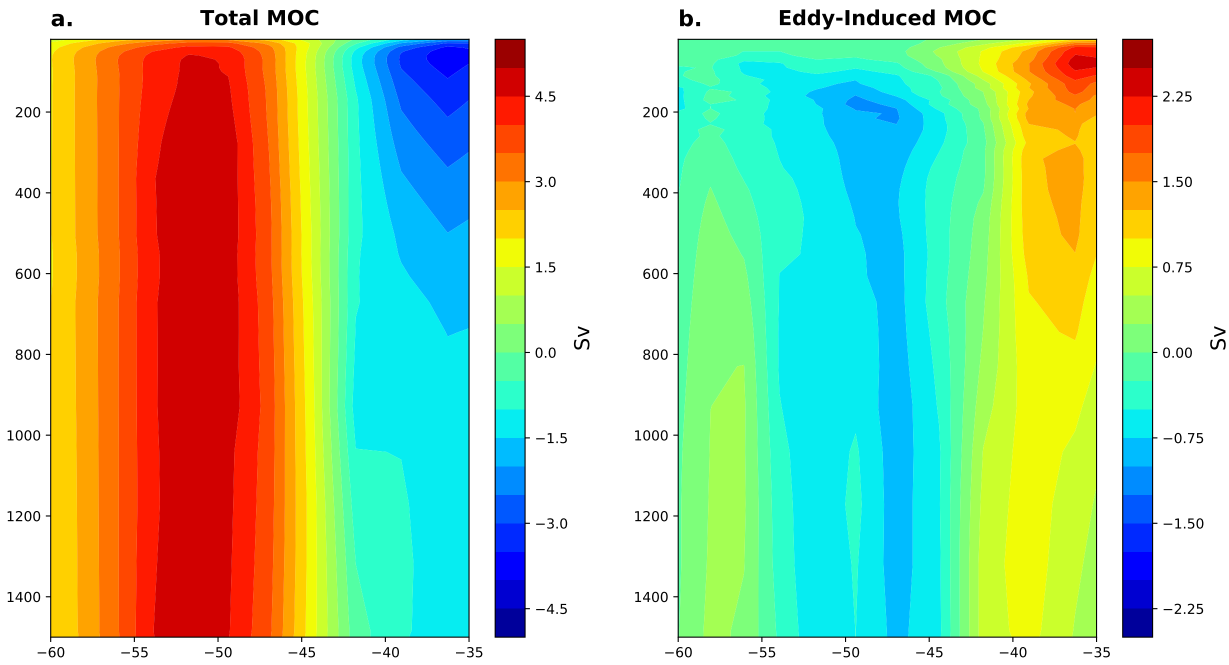

Figure S5. Precession-driven changes in (a) the Meridional Overturning Circulation (MOC) streamfunction, and (b) the eddy-induced meridional overturning streamfunction, calculated as the difference in century-means from the HighPrec and NoPrec simulations. Units are Sv, and positive streamlines indicate clockwise flow.

The Impact of Orbital Precession on Air-Sea CO_2 Exchange in the Southern Ocean

Cole F. Persch[1], **Pedro DiNezio**[1], **Nicole S. Lovenduski**[1,2]

[1]Department of Atmospheric and Oceanic Sciences, University of Colorado, Boulder, CO, USA
[2]Institute of Arctic and Alpine Research, University of Colorado, Boulder, CO, USA

Key Points:

- Increased insolation during austral summer due to orbital precession shifts the southern westerlies poleward.
- Poleward shifted westerlies enhance CO_2 outgassing due to increased turbulent exchanges and vertical transport of carbon-rich waters.
- Enhanced transport of carbon-rich waters is driven by a deepening of the overturning circulation in response to poleward shifted winds.

Corresponding author: Cole F. Persch, `cole.persch@colorado.edu`

Abstract

Orbital precession has been linked to glacial cycles and the atmospheric carbon dioxide (CO_2) concentration, yet the direct impact of precession on the carbon cycle is not well understood. We analyze output from an Earth system model configured under different orbital parameters to isolate the impact of precession on air-sea CO_2 flux in the Southern Ocean – a component of the global carbon cycle that is thought to play a key role on past atmospheric CO_2 variations. Here, we demonstrate that periods of high precession are coincident with anomalous CO_2 outgassing from the Southern Ocean. Under high precession, we find a poleward shift in the southern westerly winds, enhanced Southern Ocean meridional overturning, and an increase in the surface ocean partial pressure of CO_2 along the core of the Antarctic Circumpolar Current. These results suggest that orbital precession may have played an important role in driving changes in atmospheric CO_2.

1 Plain Language Summary

Over the past one million years, Earth has experienced several glacial and interglacial periods. As a glacial period is ending, carbon in the atmosphere can rise by up to 50%. The cause for this change is currently unknown, but most theories suggest that this carbon is released from the deep ocean into the atmosphere. The Southern Ocean surrounding Antarctica is the location of a lot of carbon outgassing from the deep ocean into the atmosphere, so it could be responsible for some of this change in atmospheric carbon. One of Earth's orbital cycles, precession, has been shown to change circulation in the Southern Ocean, that can affect how much carbon is carried from the deep ocean to the surface and released into the atmosphere. This paper uses simulations of a climate model to show that high precession corresponds to a 20% increase in the release of carbon from the Southern Ocean into the atmosphere. These findings suggest that precession could have affected changes in past atmospheric carbon concentrations.

2 Introduction

The Southern Ocean plays a central role in the global carbon cycle [*Marshall and Speer*, 2012]. The Southern Westerly Winds (SWW) interact with the ocean surface and force a zonally unbound meridional overturning circulation via Ekman transport, also known as *the Upper Cell* [*Speer et al.*, 2000]. On the poleward edge of this meridional overturning, deep, carbon-rich water is upwelled to the surface, and CO_2 is released into the atmosphere. Past studies have suggested that modern-day, interannual variability in the position and intensity of the SWW can invoke changes in Southern Ocean circulation, air-sea CO_2 flux, and atmospheric CO_2 concentration [*Lovenduski et al.*, 2007; *Butler et al.*, 2007; *Dufour et al.*, 2013; *Landschützer et al.*, 2019; *Nevison et al.*, 2020], and can influence the global carbon cycle [*Hauck et al.*, 2020].

The Southern Ocean likely played a key role in driving the large variations of atmospheric CO_2 observed over glacial-interglacial cycles [*Sigman et al.*, 2004; *Toggweiler et al.*, 2006; *Anderson et al.*, 2009]. This is because the Southern Ocean is one of the only places in the global ocean where dense ocean isopycnal surfaces outcrop, providing a means to connect the deep ocean interior to the atmosphere [*Rintoul et al.*, 2001]. However, the mechanisms responsible for changing air-sea CO_2 flux in the Southern Ocean on these timescales are not fully understood. In line with results from studies of modern-day Southern Ocean CO_2 flux variability, multiple manuscripts suggest that glacial-interglacial changes in the SWW may have played a role in some of these changes in air-sea CO_2 flux [*Toggweiler et al.*, 2006; *Menviel et al.*, 2008; *Tschumi et al.*, 2008; *Anderson et al.*, 2009; *d'Orgeville et al.*, 2010; *Lee et al.*, 2011; *Ai et al.*, 2020]. In these studies, the authors invoke SWW changes via mechanisms such as a global temperature increase [*Toggweiler et al.*, 2006], a cooling North Atlantic [*Anderson et al.*, 2009; *Lee et al.*, 2011], or variations in Earth's axial tilt (obliquity) [*Ai et al.*, 2020], yet no clear consensus on the cause of the SWW changes has emerged.

Recent studies suggest that the climate in the high-latitude Southern Hemisphere responds to orbital precession, one of the Milankovitch cycles with a spectral peak at ~21,000 years. Modelling and proxy studies have demonstrated that precession can significantly alter the position and strength of the SWW, which impacts circulation in the Southern Ocean [*Rutberg and Broccoli*, 2019; *Lamy et al.*, 2019]. Yet the models used in these studies are lacking a carbon cycle and thus are unable to predict if Southern Ocean air-sea CO_2 flux will be affected by precession.

Here, we use a state-of-the-art Earth system model which includes a respresentation of the carbon cycle to illustrate, for the first time, that orbital precession can have a marked impact on Southern Ocean air-sea CO_2 flux. We compare output from two simulations with different precessional states to illustrate the potential influence of precession on the Southern Ocean. As we will demonstrate, precession drives changes in the SWW and Southern Ocean circulation, alters the upwelling of deep, carbon-rich water, and produces anomalies in air-sea CO_2 flux. Our results suggest that orbital precession plays an important role in regulating atmospheric CO_2 concentrations, and provide a possible mechanism to explain the precessional peak in the ice core atmospheric CO_2 spectra.

3 Methods

Our primary numerical modeling tool is the low-resolution configuration of the Community Earth System Model (CESM) version 2.1.1 [*Danabasoglu et al.*, 2020], a fully coupled climate model designed for long climate integrations [*Shields et al.*, 2012]. The atmospheric component, CAM4, has a resolution of $\sim 3.75° \times 3.75°$ and 26 vertical levels [*Neale et al.*, 2013]. The ocean component, POP2, has nominal 2° latitude × 4° longitude resolution (lowering to less than 2° latitude resolution in the Southern Ocean), and 60 vertical levels [*Danabasoglu et al.*, 2012; *Smith et al.*, 2010]. POP2 represents subgrid-scale processes, such as mesoscale and submesoscale processes, via a collection of parameterizations [*Danabasoglu et al.*, 2008]. Importantly, the *Gent and Mcwilliams* [1990] mesoscale eddy parameterization includes a variable eddy-induced advection coefficient [*Gent*, 2016] which improves realism of eddy-driven mixing of carbon in the Southern Ocean at coarse resolution [*Lovenduski et al.*, 2013]. POP2 includes a biogeochemical model, MARBL [*Long et al.*, 2021]. MARBL contains multiple chemical tracers necessary for simulating ocean biogeochemistry such as carbon, nitrogen, phosphorus, iron, silicon, and oxygen.

Our experiment was designed to isolate the impact of precession on the Southern Ocean. We spun up CESM 2.1.1 for a 1000-year period with an eccentricity parameter of 0; since eccentricity modulates the strength of precession, this equilibration period had no precessional forcing. Carbon dioxide in the atmosphere is kept at a constant preindustrial value of 284.7 ppm. Over the last 500 years of the spinup, the globally integrated air-sea CO_2 flux drift is negligible ($-1.9 \pm 6.5 * 10^{-6}$ Pg C yr^{-2}; Figure S1). Following the spin-up period, two 100-year simulations were performed: the first, NoPrec, maintains an eccentricity parameter of 0, while the second, HighPrec, uses an eccentricity parameter of 0.058, which is the maximum value over the last one million years [*Laskar et al.*, 2004]. In the HighPrec simulation, the Northern Hemisphere summer solstice was configured to occur at the perihelion of Earth's orbit, which maximizes seasonal variability of insolation in the Southern Hemisphere. Our HighPrec simulation shows an immediate response of the SWW with minimal drift in global temperature consistent with the negligible effect of precession on annual mean insolation thus allowing us to use 100 years to study changes in the Southern Ocean.

While CESM2 is a well-validated model [*Danabasoglu et al.*, 2020; *Simpson et al.*, 2020; *Long et al.*, 2021], here we employ CESM2 components with lower resolution than the standard configuration, requiring an assessment of model validity at this resolution. Of particular interest in this study is the position and strength of the SWW. While the maximum zonal wind stress in the NoPrec SWW (0.14 N m^{-2}) agrees with modern estimates [*Large and Yeager*, 2009, 0.14 N m^{-2}], the modeled position of the SWW zonal wind stress (centered on 45°S) shows an equatorward bias relative to the estimated preindustrial value [*Large and Yeager*, 2009, centered on 53°S], which is a consequence of the lower resolution of the atmospheric model [*Shields et al.*, 2012]. The modelled position and strength of the SWW in our NoPrec simulation is within the range reported by models that participated in the Palaeoclimate Model Intercomparison Projects PMIP2 and PMIP3 under preindustrial conditions [*Rojas*, 2013], whose model components are simulated at a similar resolution as in our experiment. We find that the version of CESM2 employed in this study captures the air-sea fluxes of pre-industrial/natural CO_2 as compared to an observation-based inversion, as biome-mean CO_2 fluxes over the last 500 years of the spin-up simulation are within the uncertainty of the observation-based fluxes [*Mikaloff Fletcher et al.*, 2007] (Table S1).

A goal of this study is to isolate the different physical processes driving changes in air-sea CO_2 over the Southern Ocean. We approach this using the air-sea CO_2 equation as solved by the model:

$$F_{CO_2} = k_{sol} \times A_{noice} \times \Delta pCO_2 \times k_{gtv}, \tag{1}$$

where k_{sol} is the solubility of carbon in seawater, A_{noice} is the surface area without ice, ΔpCO_2 is the difference in the partial pressure of CO_2 between the surface ocean and the atmosphere, and k_{gtv} is the gas transfer velocity which is driven by surface winds [*Wanninkhof et al.*, 2013; *Wanninkhof*, 2014]. We isolate the contribution from each process as follows:

$$\delta[F]_{k_{sol}} = \delta[k_{sol}] \times A_{noice} \times \Delta pCO_2 \times k_{gtv}, \tag{2}$$

where $\delta[F]_{k_{sol}}$ isolates the impact of precession-driven changes in solubility (δk_{sol}) on air-sea CO_2 flux, δ corresponds to the difference between HighPrec and NoPrec, and the non-δ terms are derived from the NoPrec simulation.

We expanded this technique to include effects from changes in the covariance among the terms in Equation 1. Only one of these terms, the combination of ΔpCO_2 and k_{tur}, was significant relative to the changes computed using Equation 2. The influence of joint changes in these two processes was calculated as follows:

$$\delta[F]_{\Delta pCO_2, k_{gtv}} = k_{sol} \times A_{noice} \times \delta[\Delta pCO_2] \times \delta[k_{gtv}], \tag{3}$$

which isolates the impact of simultaneous, precession-driven changes in both ΔpCO_2 and k_{tur}. It is important to note that since CO_2 in the atmosphere is kept constant, the ΔpCO_2 term in the air-sea CO_2 flux decomposition corresponds to only changes in surface ocean pCO_2. The surface ocean pCO_2 changes are further broken down into contributions from temperature, salinity, Dissolved Inorganic Carbon (DIC), alkalinity, and freshwater forcing.

In this manuscript, we emphasize orbital precession-driven changes in the Southern Ocean, calculated as the difference between the century-mean values in the 100-year HighPrec simulation and the 100-year NoPrec simulation. This difference (δ) is reported to be statistically significant at the 99% level if it exceeds 2.58 times the NoPrec temporal standard deviation, assuming a normal distribution.

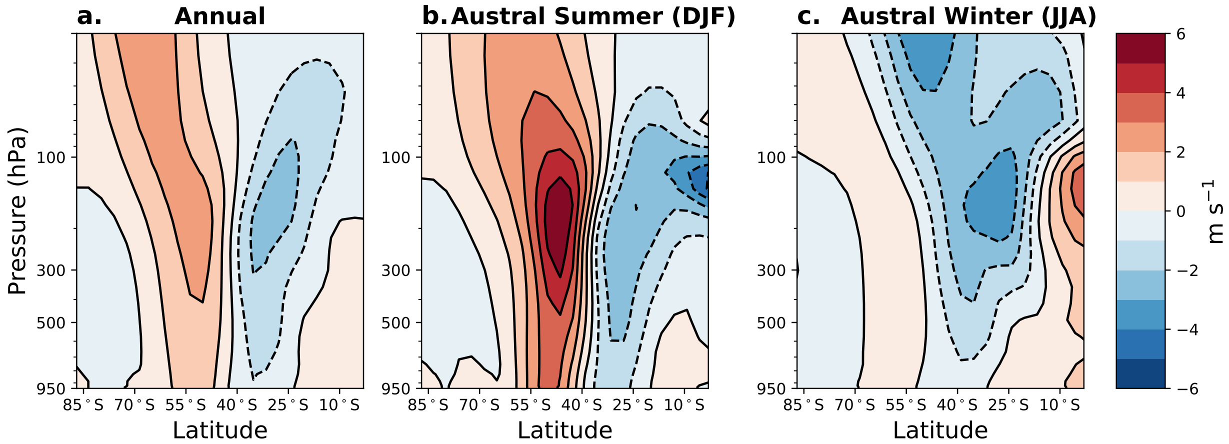

Figure 1. Precession-driven anomalies in Southern Hemisphere zonal-mean wind speed (m s^{-1}), calculated as the century-mean difference from the HighPrec and NoPrec simulations. (a) Annual-mean anomalies, (b) Austral summer (DJF) anomalies, and (c) Austral winter (JJA) anomalies. Positive values/contours correspond to westerly wind anomalies.

4 Results

Our simulations show that high precession produces a shift in the SWW that manifests most strongly in the austral summer relative to conditions with no precessional forcing. In the summer months (DJF), we find a ~6 m s^{-1} increase in the zonal-mean wind speed extending from 300 to 100 hPa and centered at 50°S; we also find a ~3 m s^{-1} decrease at the same heights centered on 30°S (Figure 1b). Whereas, in the winter months (JJA), high precession leads to a general weakening of the SWW in JJA (Figure 1c). The shift in the SWW during the DJF season exceeds the SWW weakening in the JJA season, resulting in an annual mean shift (Figure 1a). This poleward shift in the SWW appears throughout the entire vertical structure of the atmosphere, indicating a poleward intensification of the surface westerlies that drive Southern Ocean circulation.

The simulated precessional shift in the SWW corresponds to large deviations in the atmospheric temperature structure. We find that the strongest temperature anomalies occur during the DJF season, due to austral summer receiving significantly more insolation in periods of high precession (Figure S2). We find a precession-driven increase in the pole-to-Equator temperature gradient around 200 hPa in both the annual-mean and DJF zonal-mean temperature profiles (Figure S2g,h) that corresponds to the greatest wind anomalies (Figure 1a,b). These findings indicate that periods of high precession, or periods when the perihelion of Earth's orbit occur at the Southern Hemisphere summer solstice, are associated with an enhanced pole-to-Equator temperature gradient at the approximate position of the tropopause.

Carbon outgassing in the Southern Ocean increases by approximately 20% in HighPrec relative to NoPrec. The century-mean, integrated (<35°S) air-sea CO_2 flux increases from 0.264 Pg C yr^{-1} in NoPrec to 0.322 Pg C yr^{-1} in HighPrec. This precession-driven anomalous air-sea CO_2 flux is most pronounced in the Indian and Pacific sectors of the Southern Ocean: regions typically characterized by outgassing or weak uptake of CO_2 (Figure 2). North of the ACC streamlines, and in the Atlantic sector of the ACC, high precession is associated with anomalous uptake of CO_2 (Figure 2). The precession-driven anomalous outgassing exceeds the anomalous uptake, such that the Southern Ocean be-

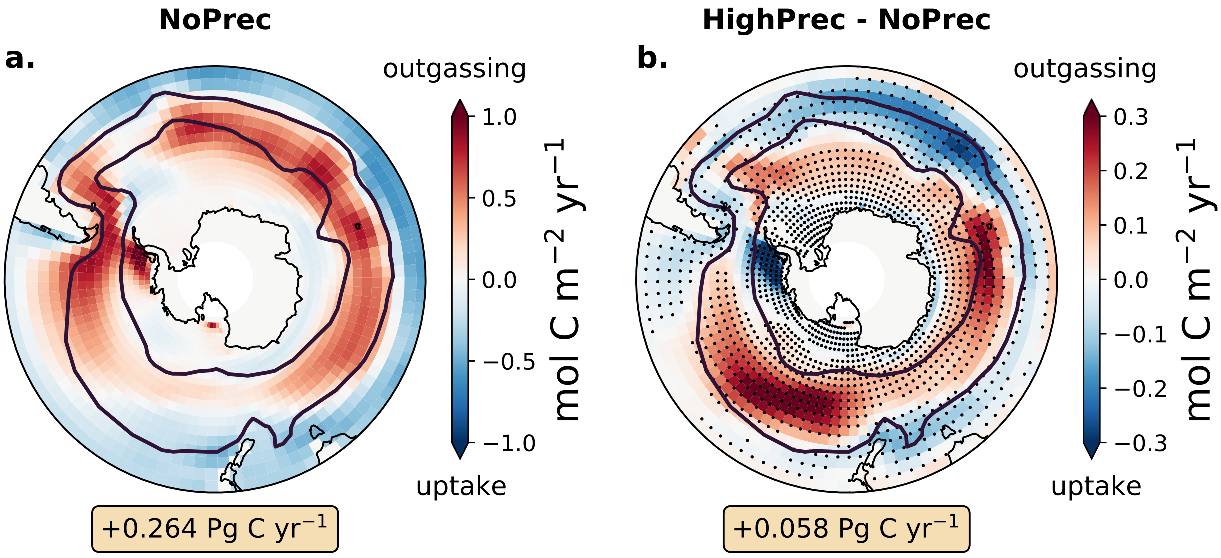

Figure 2. (a) Century-mean sea-air CO_2 flux from the NoPrec simulation. (b) Precession-driven change in sea-air CO_2 flux, calculated as the difference in century-mean CO_2 flux from the HighPrec and NoPrec simulations. Stippling indicates a statistically significant difference at the 99% confidence level. Units are mol C m^{-2} yr^{-1}, and positive values correspond to CO_2 outgassing. Black lines show the Antarctic Circumpolar Current (ACC) in the NoPrec simulation, bound by the 7 Sv and 100 Sv barotropic streamlines. Numbers under each map indicate the Southern Ocean (<35°S) integrated flux and anomalous flux, respectively (Pg C yr^{-1}).

comes a larger net source of CO_2 to the atmosphere under high precession relative to no precession.

The precession-driven increase in Southern Ocean sea-air CO_2 flux is a result of changes in both surface ocean pCO_2 and the gas transfer velocity caused by changes in precession. We isolated the influence of each physical process driving changes in air-sea flux using the technique outlined in Methods. We find that the spatial pattern of the changes in CO_2 flux is driven by the contribution from ΔpCO_2 (determined by surface ocean pCO_2 since carbon in the atmosphere is constant) (Figure 3), which itself is impacted by changing surface ocean DIC (Figure S3). This indicates that the surface ocean pCO_2 response to precession drives the anomalous outgassing in the Indian and Pacific sectors of the ACC and the anomalous uptake in the Atlantic sector of the ACC. When integrated over the Southern Ocean (<35°S), the large magnitude positive and negative ΔpCO_2 anomalies nearly balance, such that the net contribution to the integrated flux difference is small (0.019 Pg C yr^{-1}; Figure 3d). The precession-driven CO_2 flux difference is also strongly affected by the simultaneous changes in the gas transfer velocity and ΔpCO_2, which contribute to enhanced outgassing in the ACC and a large, positive Southern Ocean integrated flux contribution (0.091 Pg C yr^{-1}; Figure 3f). The changes in gas transfer velocity contributes a moderate decrease in carbon outgassing of -0.038 Pg C yr^{-1} (Figure 3e). Whereas, the changes in air-sea CO_2 flux due to sea ice extent (Figure 3b) and solubility (Figure 3c) have minimal impacts on the flux difference, with the exception of sea ice extent near the West Antarctic Peninsula which drives localized anomalous CO_2 uptake (Figure 3b).

The core of the Southern Ocean meridional overturning circulation shifts poleward and deepens under high precession, tapping into a richer carbon source explaining the

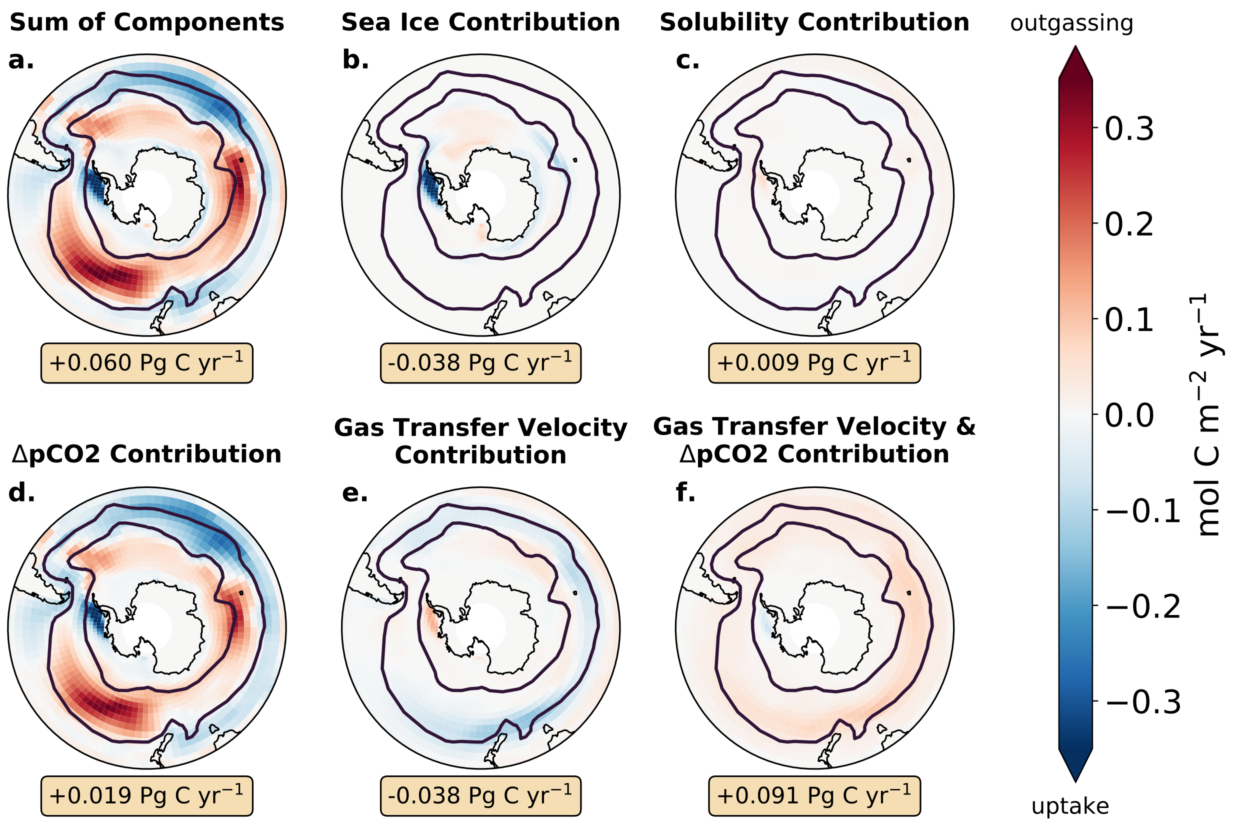

Figure 3. Contribution of (b) sea ice extent, (c) solubility, (d) ΔpCO_2, (e) gas transfer velocity, and (f) the combination of gas transfer velocity and ΔpCO_2 change to the total air-sea CO_2 flux difference (mol C m^{-2} yr^{-1}) due to precession. Contributions calculated as in Equation 2 and Equation 3 using the century-mean differences in each variable from the HighPrec and NoPrec simulations. (a) Shows the sum of the five components (b-f), which is nearly identical to Figure 2. Black lines show the Antarctic Circumpolar Current (ACC) in the NoPrec simulation, bound by the 7 Sv and 100 Sv barotropic streamlines. Numbers under each map indicate the Southern Ocean (<35°S) integrated contribution to the anomalous flux (Pg C yr^{-1}).

increase in surface pCO_2. Relative to the NoPrec simulation, both the wind stress and overturning maxima shift southward by $\sim 1°$ in the HighPrec simulation (Figure 4). In its more poleward position, the meridional overturning circulation streamlines intersect waters with higher DIC concentrations (Figure 4b). For example, the 20 Sv streamline in the NoPrec simulation intersects waters only up to 1250 meters deep with maximum DIC concentrations of $\sim$2330 mmol m^{-3}. In contrast, this streamline reaches a deeper depth of 1500 meters in the HighPrec simulation overlapping with higher DIC concentration of $\sim$2340 mmol m^{-3} (Figure 4). This shifted and deepened meridional overturning increases the amount of carbon that is brought to the surface in HighPrec relative to NoPrec, which is a key component (Figure S3) of the simulated increase in CO_2 outgassing.

The largest increases in air-sea CO_2 flux occur where precession drives both enhanced gas exchange velocities and anomalous meridional and vertical advection of carbon-rich water (Figures 2, 3, 4, S4). High precession is associated with increases in the modeled air-sea gas transfer velocity, k_{gtv}, near the northern core of the ACC; these increases are especially pronounced in the Indian and western Pacific sectors (Figure S4)a). The SWW changes that induce increases in near surface turbulence and air-sea gas exchange also alter the ocean circulation (Figure 4), driving increases in surface ocean DIC and pCO_2 in the Indian and western Pacific sectors of the ACC (Figures S4b, S3a). Where the gas transfer velocity and pCO_2 anomalies align, they combine to produce enhanced CO_2 outgassing (Figures 2b, 4).

5 Conclusions and Discussion

Our study demonstrates that high precessional states impact key Southern Ocean processes involved in the global carbon cycle, ultimately leading to a substantial increase in sea-air CO_2 flux. Under high precessional forcing of the Southern Hemisphere, our model predicts a $\sim 1°$ poleward shift of the SWW across the troposphere, likely caused by insolation-driven atmospheric temperature changes over Antarctica. The associated poleward shift in the SWW drives a stronger and deeper meridional overturning circulation, enhancing the vertical and lateral advection of carbon-rich water. The shifted SWW also increase turbulent air-sea exchange which combined with the changes ocean overturning combine to produce a 20% increase in CO_2 outgassing from the Southern Ocean.

The precession-driven poleward shift in the SWW predicted by our model strongly resembles a positive phase of the Southern Annular Mode [SAM; see, e.g., Figure 7 of *Thompson et al.*, 2000], albeit with a different seasonality. While the SAM pattern has been linked to internal climate variability and anthropogenic forcing, here we demonstrate that the Southern Hemisphere seasonal insolation changes associated with precession produce a similar shift in the SWW. The simulated change in the equator-to-pole temperature gradient in the upper troposphere is similar to that of the positive SAM phase, when the polar atmosphere shows cooling aloft associated with Ozone forcing [see Figure 8 of *Thompson et al.*, 2000]. Periods of high precession shift and deepen the meridional overturning circulation in our model (Figure 4b), which has also been found to occur during positive phases of the SAM [*Yang et al.*, 2007]. Thus, results from our simulations suggest that the Southern Hemisphere response to precessional forcing exhibits similar features to the Southern Hemisphere response to variability associated with the SAM, suggesting that past changes could be used to understand ongoing changes in Southern Hemisphere climate.

The precession-driven changes in ocean meridional overturning and air-sea CO_2 flux that we report broadly agree with other modeling studies that directly test the response of the Southern Ocean to changes in the magnitude and position of the SWWs [*Menviel et al.*, 2008; *Tschumi et al.*, 2008; *d'Orgeville et al.*, 2010]. While these studies are focused on shifts in the winds caused by a combination of orbital forcing changes on glacial-

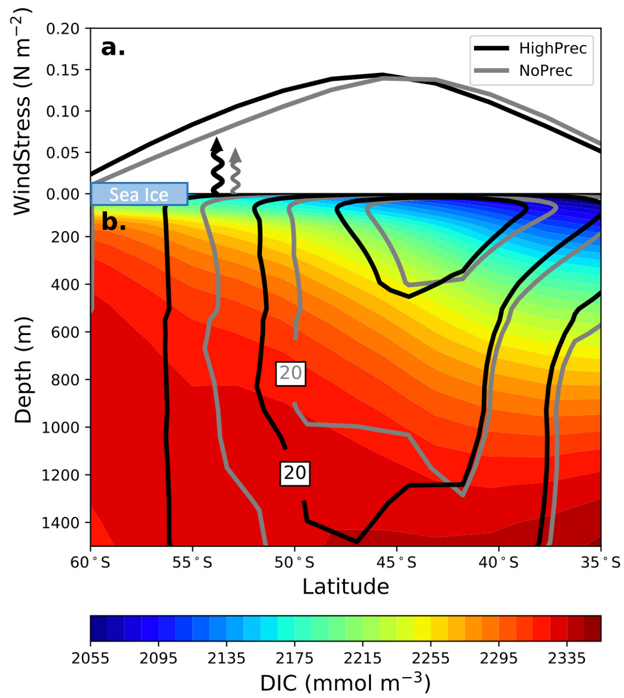

Figure 4. Southern Ocean response to high precession. (a) Century-mean zonal-mean surface wind stress from (gray) the NoPrec simulation and (black) the HighPrec simulation. (b) Century-mean (colors) zonal-mean DIC concentration from the HighPrec simulation with meridional overturning streamlines from the (gray) NoPrec simulation and (black) HighPrec simulation. Overturning units are Sv with contour lines every 10 Sv; positive streamlines indicate clockwise flow. Squiggly arrows indicate the relative position and strength in the annual peak carbon outgassing in both simulations.

to-interglacial timescales, our study demonstrates that orbital precession alone can induce changes in the SWW and thus air-sea CO_2 flux.

Our study uses an Earth system model that is configured with relatively coarse horizontal resolution in the atmosphere and ocean model components to support long integrations potentially affect the realism of our results. The average annual peak in zonal-mean wind stress occurs at 45°S in our model. While this shows good agreement with other models that have similar horizontal resolution [see Figure 3 of *Shields et al.*, 2012], this position is equatorward relatove to the modern-day position of 53° *Large and Yeager* [2009]. Similar poleward shift in the position of the SWW in response to high precession is also found in other modeling studies with higher resolution, suggesting our results are not model dependent For instance, *Rutberg and Broccoli* [2019] used a model with a resolution of 2° latitude by 2.5° longitude in the atmosphere and found a poleward shift of 4° between extreme precessional states. The coarse resolution of our ocean model component requires that processes influenced by mesoscale eddies are parameterized. Numerous studies have emphasized the importance of mesoscale eddies in Southern Ocean meridional overturning, especially in its response to changes in surface wind stress [*Marshall and Radko*, 2003; *Hallberg and Gnanadesikan*, 2006; *Abernathey et al.*, 2011; *Marshall and Speer*, 2012; *Doddridge et al.*, 2019]. Our model uses a variable eddy-induced advection coefficient [*Gent*, 2016], which has been shown to capture the sensitivity of these unresolved processes to changes in circulation [*Lovenduski et al.*, 2013]. Indeed, results from our model indicate that the eddy-induced meridional overturning circulation strengthens in response to SWW changes under high precession (counterclockwise anomalies in Figure S5b), suggesting that our coarse resolution ocean model component is capable of capturing changes in unresolved eddy advection. Future work should explore the responses identified here using higher resolution configuration of capable of resolving these processes.

Taken together, our findings imply that orbital precession plays an important role in regulating atmospheric carbon dioxide concentration through its effect on the Southern Ocean. While our study is focused on the impact of precession on Southern Ocean CO_2 fluxes, it is reasonable to expect that other regions in the coupled, global Earth system could also be affected by changes in precession. Future studies should address whether precession produces anomalous air-sea CO_2 fluxes in other regions of the global ocean, and whether the global ocean carbon reservoir grows or shrinks in response to precession. As we have demonstrated, the changes in seasonal insolation associated with orbital precession could have driven to a shift in the position of the westerly winds over the Southern Ocean, increasing the upwelling of carbon-rich water to the surface exchanging more carbon with the atmosphere. This mechanism could explain variability in ice core records of atmospheric CO_2 variability on precessional timescales [*Petit et al.*, 1999].

Open Research

The analysis data of the CESM simulation in this study were uploaded to https://doi.org/10.5281/zenodo.7761019.

Acknowledgments

This research was supported by the National Science Foundation (OCE-2043447 to PD and CP and OCE-1752724, OCE-1948664, and FRES-2021648 to NL). NCAR is sponsored by the National Science Foundation. Computational facilities have been provided by the Climate Simulation Laboratory, which is managed by CISL at NCAR.

References

Abernathey, R., J. Marshall, and D. Ferreira (2011), The dependence of southern ocean meridional overturning on wind stress, *Journal of Physical Oceanography*, *41*(12), 2261–2278.

Ai, X. E., A. S. Studer, D. M. Sigman, A. Martínez-García, F. Fripiat, L. M. Thöle, E. Michel, J. Gottschalk, L. Arnold, S. Moretti, et al. (2020), Southern ocean upwelling, earth's obliquity, and glacial-interglacial atmospheric co2 change, *Science*, *370*(6522), 1348–1352.

Anderson, R., S. Ali, L. Bradtmiller, S. Nielsen, M. Fleisher, B. Anderson, and L. Burckle (2009), Wind-driven upwelling in the southern ocean and the deglacial rise in atmospheric co2, *science*, *323*(5920), 1443–1448.

Butler, A. H., D. W. Thompson, and K. R. Gurney (2007), Observed relationships between the southern annular mode and atmospheric carbon dioxide, *Global Biogeochemical Cycles*, *21*(4).

Danabasoglu, G., R. Ferrari, and J. C. McWilliams (2008), Sensitivity of an ocean general circulation model to a parameterization of near-surface eddy fluxes, *Journal of Climate*, *21*(6), 1192–1208.

Danabasoglu, G., S. C. Bates, B. P. Briegleb, S. R. Jayne, M. Jochum, W. G. Large, S. Peacock, and S. G. Yeager (2012), The ccsm4 ocean component, *Journal of Climate*, *25*(5), 1361–1389.

Danabasoglu, G., J.-F. Lamarque, J. Bacmeister, D. Bailey, A. DuVivier, J. Edwards, L. Emmons, J. Fasullo, R. Garcia, A. Gettelman, et al. (2020), The community earth system model version 2 (cesm2), *Journal of Advances in Modeling Earth Systems*, *12*(2), e2019MS001,916.

Doddridge, E. W., J. Marshall, H. Song, J.-M. Campin, M. Kelley, and L. Nazarenko (2019), Eddy compensation dampens southern ocean sea surface temperature response to westerly wind trends, *Geophysical Research Letters*, *46*(8), 4365–4377.

d'Orgeville, M., W. Sijp, M. England, and K. Meissner (2010), On the control of glacial-interglacial atmospheric co2 variations by the southern hemisphere westerlies, *Geophysical Research Letters*, *37*(21).

Dufour, C. O., J. L. Sommer, M. Gehlen, J. C. Orr, J.-m. Molines, J. Simeon, and B. Barnier (2013), Eddy compensation and controls of the enhanced sea-to-air co2 flux during positive phases of the southern annular mode, *Global Biogeochemical Cycles*, *27*(3), 950–961.

Gent, P. R. (2016), Effects of southern hemisphere wind changes on the meridional overturning circulation in ocean models, *Annual review of marine science*, *8*, 79–94.

Gent, P. R., and J. C. Mcwilliams (1990), Isopycnal mixing in ocean circulation models, *Journal of Physical Oceanography*, *20*(1), 150–155.

Hallberg, R., and A. Gnanadesikan (2006), The role of eddies in determining the structure and response of the wind-driven southern hemisphere overturning: Results from the modeling eddies in the southern ocean (meso) project, *Journal of Physical Oceanography*, *36*(12), 2232–2252.

Hauck, J., M. Zeising, C. Le Quéré, N. Gruber, D. C. Bakker, L. Bopp, T. T. T. Chau, Ö. Gürses, T. Ilyina, P. Landschützer, et al. (2020), Consistency and challenges in the ocean carbon sink estimate for the global carbon budget, *Frontiers in Marine Science*, *7*, 571,720.

Lamy, F., J. C. Chiang, G. Martínez-Méndez, M. Thierens, H. W. Arz, J. Bosmans, D. Hebbeln, F. Lambert, L. Lembke-Jene, and J.-B. Stuut (2019), Precession modulation of the south pacific westerly wind belt over the past million years, *Proceedings of the National Academy of Sciences*, *116*(47), 23,455–23,460.

Landschützer, P., T. Ilyina, and N. S. Lovenduski (2019), Detecting regional modes of variability in observation-based surface ocean p co2, *Geophysical Research Let-*

ters, *46*(5), 2670–2679.
Large, W., and S. Yeager (2009), The global climatology of an interannually varying air–sea flux data set, *Climate dynamics*, *33*, 341–364.
Laskar, J., P. Robutel, F. Joutel, M. Gastineau, A. Correia, and B. Levrard (2004), A long-term numerical solution for the insolation quantities of the earth, *Astronomy & Astrophysics*, *428*(1), 261–285.
Lee, S.-Y., J. C. Chiang, K. Matsumoto, and K. S. Tokos (2011), Southern ocean wind response to north atlantic cooling and the rise in atmospheric co2: Modeling perspective and paleoceanographic implications, *Paleoceanography*, *26*(1).
Long, M. C., J. K. Moore, K. Lindsay, M. Levy, S. C. Doney, J. Y. Luo, K. M. Krumhardt, R. T. Letscher, M. Grover, and Z. T. Sylvester (2021), Simulations with the marine biogeochemistry library (marbl), *Journal of Advances in Modeling Earth Systems*, *13*(12), e2021MS002,647.
Lovenduski, N. S., N. Gruber, S. C. Doney, and I. D. Lima (2007), Enhanced co2 outgassing in the southern ocean from a positive phase of the southern annular mode, *Global Biogeochemical Cycles*, *21*(2).
Lovenduski, N. S., M. C. Long, P. R. Gent, and K. Lindsay (2013), Multi-decadal trends in the advection and mixing of natural carbon in the southern ocean, *Geophysical Research Letters*, *40*(1), 139–142.
Marshall, J., and T. Radko (2003), Residual-mean solutions for the antarctic circumpolar current and its associated overturning circulation, *Journal of Physical Oceanography*, *33*(11), 2341–2354.
Marshall, J., and K. Speer (2012), Closure of the meridional overturning circulation through southern ocean upwelling, *Nature Geoscience*, *5*(3), 171–180.
Menviel, L., A. Timmermann, A. Mouchet, and O. Timm (2008), Climate and marine carbon cycle response to changes in the strength of the southern hemispheric westerlies, *Paleoceanography*, *23*(4).
Mikaloff Fletcher, S., N. Gruber, A. R. Jacobson, M. Gloor, S. Doney, S. Dutkiewicz, M. Gerber, M. Follows, F. Joos, K. Lindsay, et al. (2007), Inverse estimates of the oceanic sources and sinks of natural co2 and the implied oceanic carbon transport, *Global Biogeochemical Cycles*, *21*(1).
Neale, R. B., J. Richter, S. Park, P. H. Lauritzen, S. J. Vavrus, P. J. Rasch, and M. Zhang (2013), The mean climate of the community atmosphere model (cam4) in forced sst and fully coupled experiments, *Journal of Climate*, *26*(14), 5150–5168.
Nevison, C. D., D. R. Munro, N. S. Lovenduski, R. F. Keeling, M. Manizza, E. J. Morgan, and C. Rödenbeck (2020), Southern annular mode influence on wintertime ventilation of the southern ocean detected in atmospheric o2 and co2 measurements, *Geophysical Research Letters*, *47*(4), e2019GL085,667.
Petit, J.-R., J. Jouzel, D. Raynaud, N. I. Barkov, J.-M. Barnola, I. Basile, M. Bender, J. Chappellaz, M. Davis, G. Delaygue, et al. (1999), Climate and atmospheric history of the past 420,000 years from the vostok ice core, antarctica, *Nature*, *399*(6735), 429–436.
Rintoul, S. R., C. W. Hughes, and D. Olbers (2001), The antarctic circumpolar current system, in *International Geophysics*, vol. 77, pp. 271–XXXVI, Elsevier.
Rojas, M. (2013), Sensitivity of southern hemisphere circulation to lgm and 4× co2 climates, *Geophysical Research Letters*, *40*(5), 965–970.
Rutberg, R., and A. Broccoli (2019), Response of the high-latitude southern hemisphere to precessional forcing: Implications for pleistocene ocean circulation, *Paleoceanography and paleoclimatology*, *34*(7), 1092–1106.
Shields, C. A., D. A. Bailey, G. Danabasoglu, M. Jochum, J. T. Kiehl, S. Levis, and S. Park (2012), The low-resolution ccsm4, *Journal of Climate*, *25*(12), 3993–4014.
Sigman, D. M., S. L. Jaccard, and G. H. Haug (2004), Polar ocean stratification in a cold climate, *Nature*, *428*(6978), 59–63.

Simpson, I. R., J. Bacmeister, R. B. Neale, C. Hannay, A. Gettelman, R. R. Garcia, P. H. Lauritzen, D. R. Marsh, M. J. Mills, B. Medeiros, et al. (2020), An evaluation of the large-scale atmospheric circulation and its variability in cesm2 and other cmip models, *Journal of Geophysical Research: Atmospheres*, *125*(13), e2020JD032,835.

Smith, R., P. Jones, B. Briegleb, F. Bryan, G. Danabasoglu, J. Dennis, J. Dukowicz, C. Eden, B. Fox-Kemper, P. Gent, et al. (2010), The parallel ocean program (pop) reference manual ocean component of the community climate system model (ccsm) and community earth system model (cesm), *LAUR-01853*, *141*, 1–140.

Speer, K., S. R. Rintoul, and B. Sloyan (2000), The diabatic deacon cell, *Journal of physical oceanography*, *30*(12), 3212–3222.

Thompson, D. W., J. M. Wallace, and G. C. Hegerl (2000), Annular modes in the extratropical circulation. part ii: Trends, *Journal of climate*, *13*(5), 1018–1036.

Toggweiler, J. R., J. L. Russell, and S. R. Carson (2006), Midlatitude westerlies, atmospheric co2, and climate change during the ice ages, *Paleoceanography*, *21*(2).

Tschumi, T., F. Joos, and P. Parekh (2008), How important are southern hemisphere wind changes for low glacial carbon dioxide? a model study, *Paleoceanography*, *23*(4).

Wanninkhof, R. (2014), Relationship between wind speed and gas exchange over the ocean revisited, *Limnology and Oceanography: Methods*, *12*(6), 351–362.

Wanninkhof, R., G.-H. Park, T. Takahashi, C. Sweeney, R. Feely, Y. Nojiri, N. Gruber, S. C. Doney, G. A. McKinley, A. Lenton, et al. (2013), Global ocean carbon uptake: magnitude, variability and trends, *Biogeosciences*, *10*(3), 1983–2000.

Yang, X.-Y., D. Wang, J. Wang, and R. X. Huang (2007), Connection between the decadal variability in the southern ocean circulation and the southern annular mode, *Geophysical Research Letters*, *34*(16).

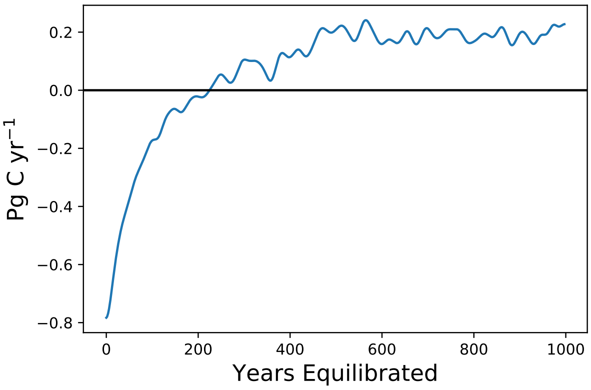

Figure S1. Globally integrated sea-air CO_2 flux during the model spin-up. High-frequency variability has been removed using a σ=10 Gaussian filter.

Region	Model spin-up	*Mikaloff Fletcher et al.* [2007]
Polar S. Ocean	0.10 ±0.03	0.04 ±0.04
Sub-Polar Pac. & Ind.	0.31 ±0.08	0.25 ±0.09
Sub-Polar Atl.	0.11 ±0.03	0.11 ±0.05

Table S1. Spatially integrated air-sea CO_2 flux (Pg C yr^{-1}) in three Southern Ocean regions averaged over the last 500 years of the model spin-up, and the natural air-sea CO_2 flux reported in *Mikaloff Fletcher et al.* [2007].

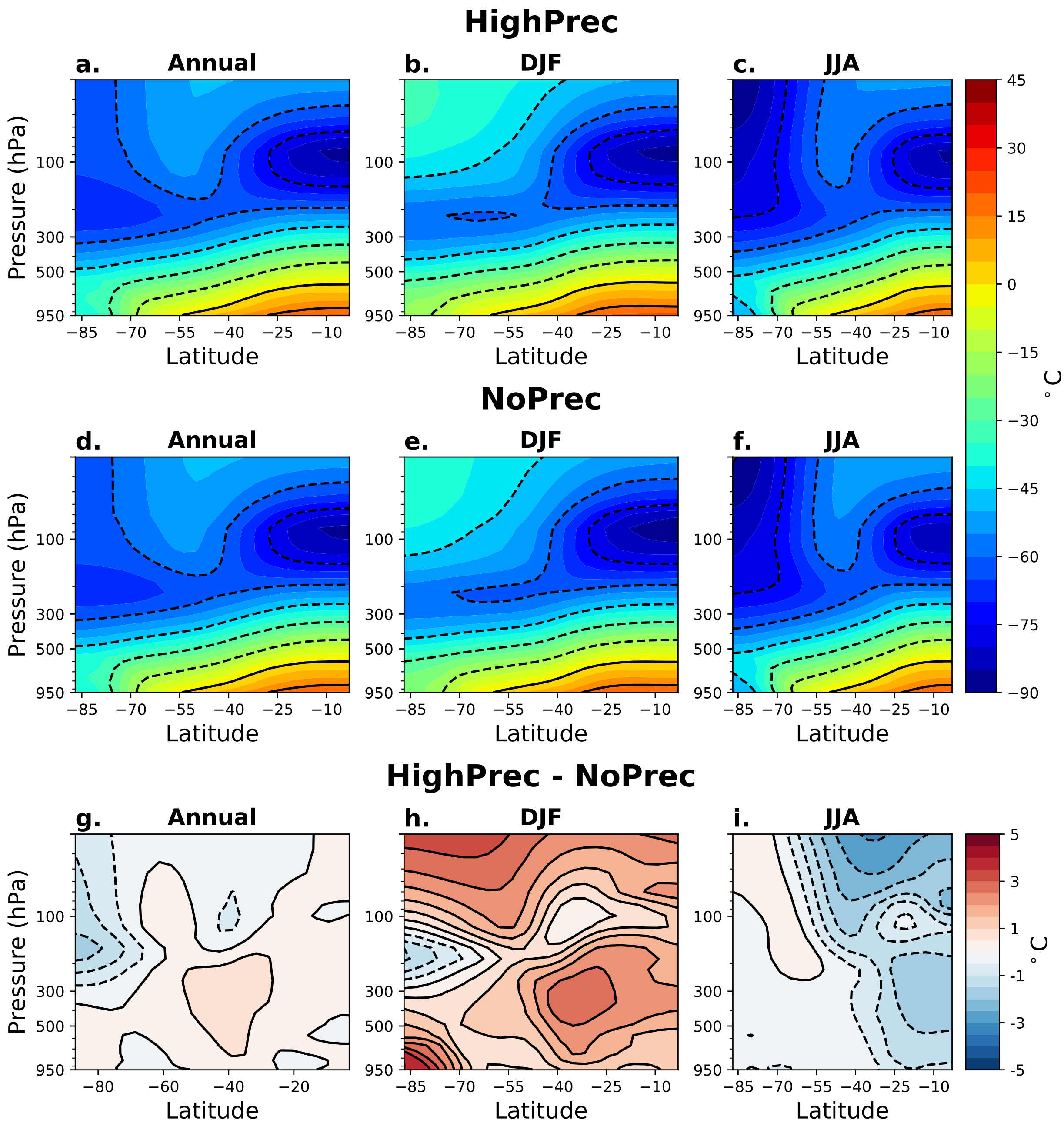

Figure S2. Zonal-mean atmospheric temperature for (1^{st} column) annual-mean, (2^{nd} column) Austral summer (DJF), and (3^{rd} column) Austral winter (JJA) periods in the (1^{st} row) HiPrec and (2^{nd} row) NoPrec simulations (°C). (3^{rd} row) Precession-driven anomalies in zonal-mean atmospheric temperature, calculated as the century-mean difference from the HighPrec and NoPrec simulations.

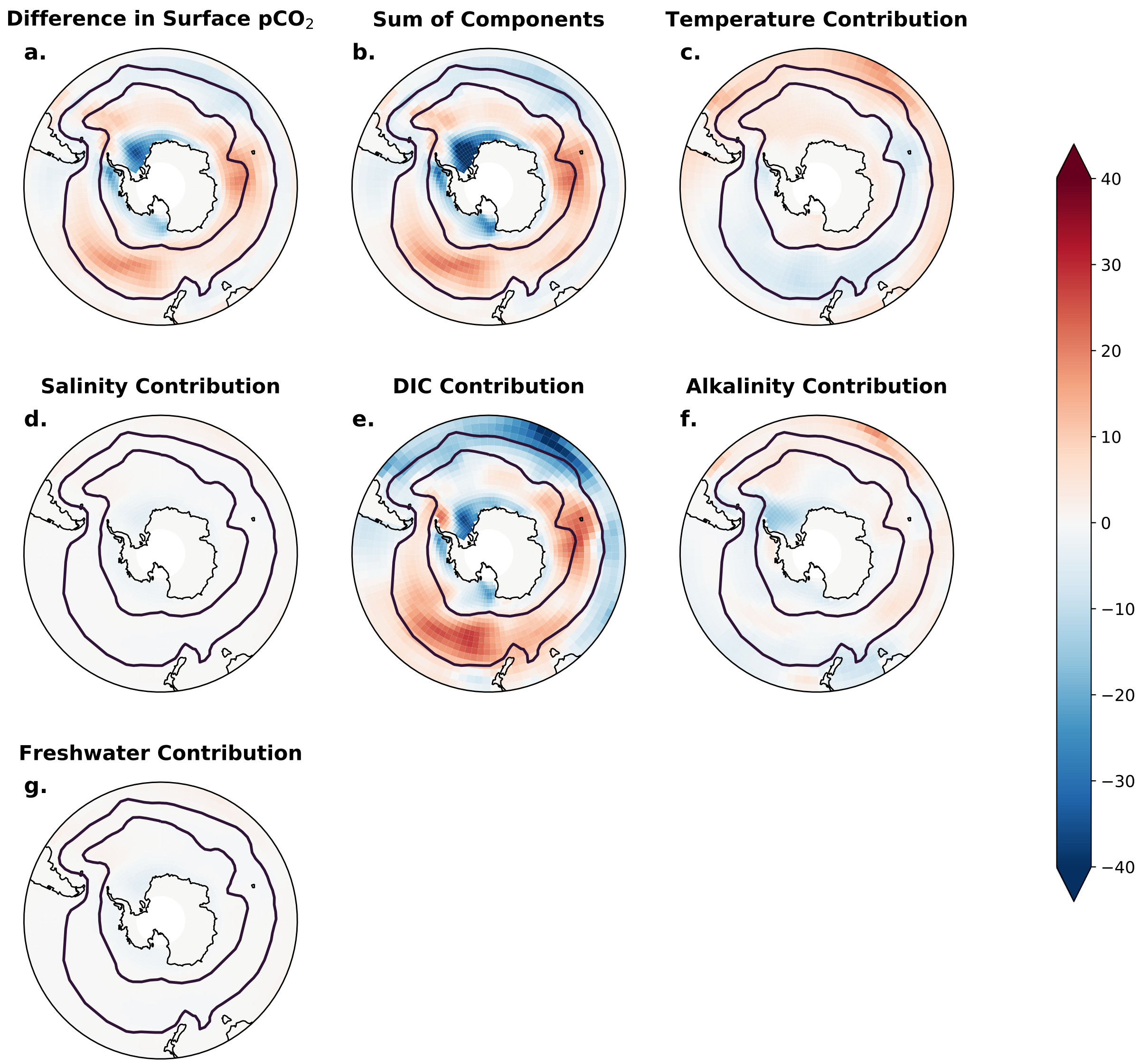

Figure S3. Contribution of (c) temperature, (d) salinity, (e) DIC, (e) Alkalinity, and (f) freshwater anomalies to the total surface ocean pCO_2 (ppmv) difference due to precession. The contributions of each variable responsible for driving surface ocean pCO_2 were calculated using the century-mean differences in each variable from the HighPrec and NoPrec simulations [see Equation 3 of *Lovenduski et al.*, 2007]. (b) Shows the sum of the five components (c-g). Black lines show the Antarctic Circumpolar Current (ACC) in the NoPrec simulation, bound by the 7 Sv and 100 Sv barotropic streamlines.

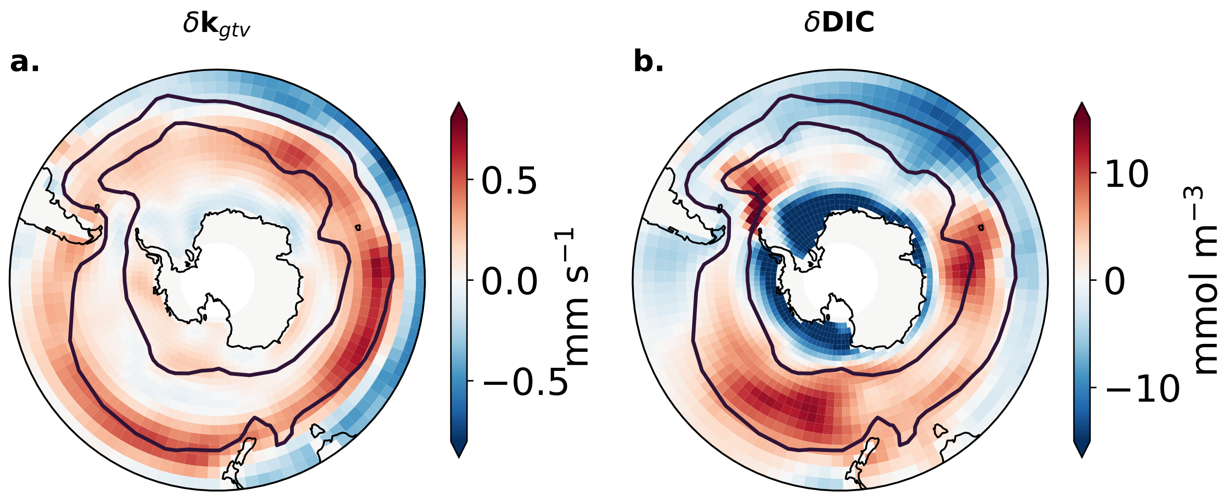

Figure S4. Precession-driven changes in (a) air-sea gas transfer velocity (mm s^{-1}), and (b) surface ocean DIC (mmol m^{-3}), calculated as the difference in century-means from the HighPrec and NoPrec simulations. Black lines show the Antarctic Circumpolar Current (ACC) in the NoPrec simulation, bound by the 7 Sv and 100 Sv barotropic streamlines.

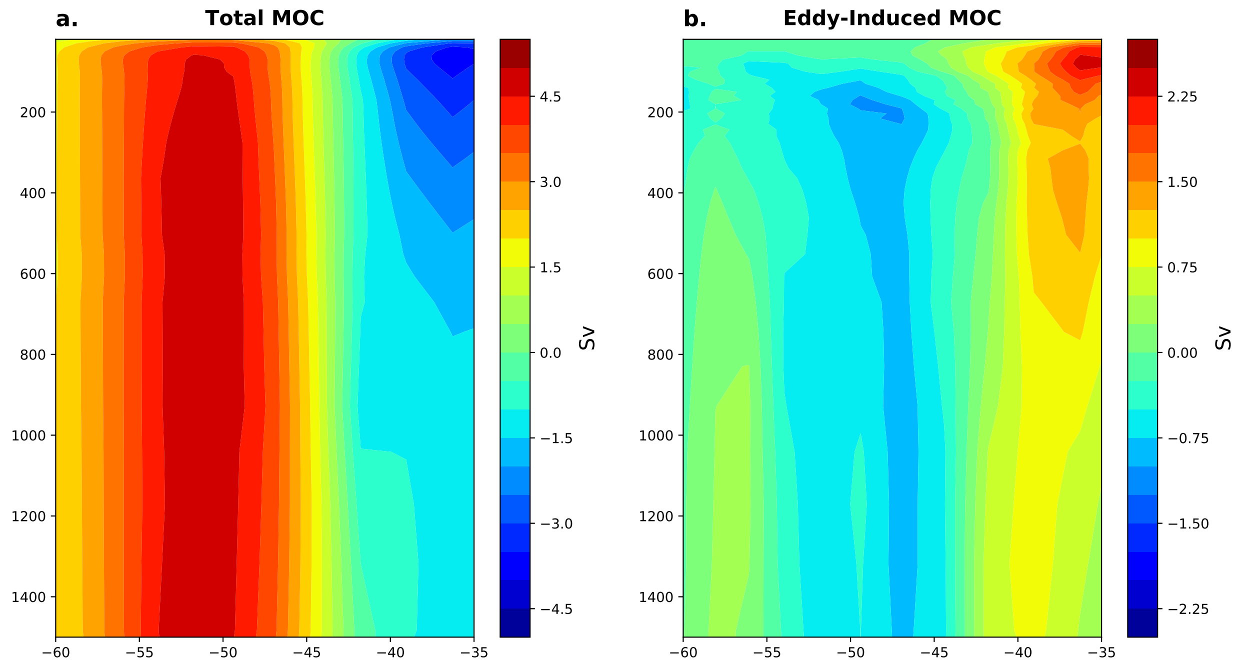

Figure S5. Precession-driven changes in (a) the Meridional Overturning Circulation (MOC) streamfunction, and (b) the eddy-induced meridional overturning streamfunction, calculated as the difference in century-means from the HighPrec and NoPrec simulations. Units are Sv, and positive streamlines indicate clockwise flow.